DIRECTION FINDING WITH TDOA IN A MULTIPATH LAND ENVIRONMENT

A THESIS SUBMITTED TO
THE GRADUATE SCHOOL OF NATURAL AND APPLIED SCIENCES
OF
MIDDLE EAST TECHNICAL UNIVERSITY

BY

ÇAĞRI HALİS BAŞÇİFTÇİ

IN PARTIAL FULLFILLMENT OF THE REQUIREMENTS
FOR
THE DEGREE OF MASTER OF SCIENCE
IN
ELECTRICAL AND ELECTRONICS ENGINEERING

SEPTEMBER 2007

Approval of the Thesis:

DIRECTION FINDING WITH TDOA IN A MULTIPATH LAND ENVIRONMENT

submitted by **ÇAĞRI HALİS BAŞÇİFTÇİ** in partial fulfillment of the requirements for the degree of **Master of Science in Electrical and Electronics Engineering Department, Middle East Technical University** by,

Prof. Dr. Canan Özgen _____
Dean, Graduate School of **Natural and Applied Sciences**

Prof. Dr. İsmet Erkmen _____
Head of Department, **Electrical and Electronics Engineering**

Assoc. Prof. Dr. Sencer Koç _____
Supervisor, **Electrical and Electronics Engineering Dept., METU**

Prof. Dr. Yalçın Tanık _____
Co-Supervisor, **Electrical and Electronics Engineering Dept., METU**

Examining Committee Members:

Prof. Dr. Mustafa Kuzuoğlu _____
Electrical and Electronics Engineering Dept., METU

Assoc. Prof. Dr. Sencer Koç _____
Electrical and Electronics Engineering Dept., METU

Prof. Dr. Yalçın Tanık _____
Electrical and Electronics Engineering Dept., METU

Assist. Prof. Dr. Ali Özgür Yılmaz _____
Electrical and Electronics Engineering Dept., METU

Dr. Toygar Birinci _____
ASELSAN

Date: _____

I hereby declare that all information in this document has been obtained and presented in accordance with academic rules and ethical conduct. I also declare that, as required by these rules and conduct, I have fully cited and referenced all material and results that are not original to this work.

Name, Last name : Çağrı Halis Başçiftçi

Signature :

ABSTRACT

DIRECTION FINDING WITH TDOA IN A MULTIPATH LAND ENVIRONMENT

Başçiftçi, Çağrı Halis

M.S., Department of Electrical and Electronics Engineering

Supervisor : Assoc. Prof. Dr. Sencer Koç

Co-Supervisor : Prof. Dr. Yalçın Tanık

September 2007, 98 pages

In this thesis, the problem of Angle of Arrival estimation of radar signals with Time Difference of Arrival method in an outdoor land multipath environment with limited line of sight is analyzed. A system model is proposed. Effects of system, channel and radar parameters on the Angle of Arrival estimation performance are investigated through Monte Carlo simulations.

Improving effect of utilization of diversity on the estimation performance is observed. Performances of the space diversity with noncoherent and selective combining are compared.

Finally a realistic scenario is studied and performance of the proposed system is investigated.

Keywords: Angle of Arrival, Time Difference of Arrival, Direction Finding, Multipath Channel, Diversity

ÖZ

VZFPÖ YÖNTEMİ İLE ÇOKYOLLU KARA ORTAMINDA YÖN KESTİRİMİ

Başçiftçi, Çağrı Halis

Yüksek Lisans, Elektrik Elektronik Mühendisliği Bölümü

Tez Yöneticisi : Doç. Dr. Sencer Koç

Ortak Tez Yöneticisi: Prof. Dr. Yalçın Tanık

Eylül 2007, 98 sayfa

Bu tezde, açık alanda görüş hattı kısıtlı yansımalı bir kara ortamında varış zamanları farkının pasif ölçümü yöntemi ile radar sinyallerinin varış açısının kestirimi ele alınmıştır. Bir yön bulma sistemi modeli önerilmiştir. Sistem, kanal ve radar değişkenlerinin, kestirim başarımı üzerine etkileri Monte Carlo benzetimleri ile incelemiştir.

Çeşitlemenin kestirim başarımı üzerine iyileştirici etkileri incelenmiştir. Uzamsal evreuyumsuz birleştirici çeşitleme ile seçici çeşitlemenin başarımları karşılaştırılmıştır.

Son olarak bir gerçek hayat yön bulma senaryosu çalışılmış ve önerilen sistemin bu senaryodaki başarımı incelemiştir.

Anahtar Kelimeler: Varış Açısı, Varış Zamanları Farkı, Yön Bulma, Çokyollu Kanal, Çeşitleme

To My Parents

ACKNOWLEDGEMENTS

I would like to express my sincere gratitude to my supervisors Dr. Sencer Koç and Dr. Yalçın Tanık, for their keen interest, guidance, endless patience, and support during this work. Without their support and guidance this thesis would not be possible.

I also want to thank to my colleagues in ASELSAN for their support. Moreover, I am thankful to my company ASELSAN for letting and supporting my thesis.

The last but not least I would like to express my thanks to my family for their irresistible insistence, encouragement and sacrifice during the completion of this thesis.

TABLE OF CONTENTS

APPENDICES

LIST OF TABLES

LIST OF FIGURES

LIST OF ABBREVIATIONS

AMDF	Average Magnitude Difference Function
A/D	Analog to Digital
AOA	Angle of Arrival
BW	Bandwidth
CC	Crosscorrelation
CRLB	Cramer Rao Lower Bound
DF	Direction Finding
DOA	Direction of Arrival
EGC	Equal Gain Combining
EW	Electronic Warfare
FIR	Finite Impulse Response
GCC	Generalized Crosscorrelation
GPS	Global Positioning System
IF	Intermediate Frequency
LE	Leading Edge
LMS	Least Mean Square
LOS	Line of Sight
LPF	Low Pass Filter
LTI	Linear Time Invariant
LTV	Linear Time Varying
MAP	Maximum A Posteriori
MRC	Maximal Ratio Combining
MSE	Mean Square Error
NC	Noncoherent Combining
NLOS	Non Line of Sight
PHAT	Phase Transform

PW	Pulsewidth
SC	Selective Combining
SNR	Signal to Noise Ratio
SCOT	Smoothed Coherence Transform
RMS	Root Mean Square
RF	Radio Frequency
TDOA	Time Difference of Arrival
TOA	Time of Arrival
WSSUS	Wide Sense Stationary Uncorrelated Scattering

CHAPTER 1

INTRODUCTION

1.1 Scope and Objective

The objective of this thesis is investigation of AOA estimation of a radar signal with monopulse TDOA in a multipath land environment with limited LOS. Determining the AOA of a signal is fundamental to electronic intelligence, because the AOA is a parameter that hostile agile signal emitters cannot change on a pulse-to-pulse basis. Therefore measuring the emitter's bearing has the importance as an invariant sorting parameter in the deinterleaving of agile pulsed radar signals. Since Monopulse AOA estimation techniques find the AOA of radar signal from a single radar pulse, they are very crucial for EW applications [1], [2]. Monopulse techniques in the literature are amplitude comparison, phase comparison, amplitude-phase comparison and Monopulse TDOA.

Environment in which a land based DF system is located, affects its AOA estimation performance. Although Monopulse techniques such as amplitude comparison and phase comparison are known to be successful at single path environments, they fail in multipath environments, [2]. On the other hand TDOA is known to have promising performance in indoor reverberant environments to some extent, [3]. Performance of TDOA in an outdoor land environment is not studied in the literature to the best of our knowledge.

In order to estimate TDOA between received signals, possible methods proposed in the literature are GCC, adaptive algorithms and LE TDOA. For selecting the required TDOA estimation method following criteria have to be satisfied:

1. TDOA method has to be suitable for Monopulse applications
2. TDOA method has to be immune to the effects of multipath environment

Adaptive algorithms minimize the mean square error between received signals iteratively for TDOA estimation, [4]. Although they have promising results in multipath environments, due to their long convergence times they are not applicable for Monopulse TDOA, [5].

LE TDOA method measures the arrival time of the radar pulse at an interception receiver and the difference between arrival times of the same pulse at two separated sensor yield TDOA, [6]. LE TDOA method is suitable for Monopulse. On the other hand usage of LE TDOA is limited to single path environments since the leading edge of the pulse is distorted in multipath environment if the tap intervals of the channel are on the order of the duration of leading edge of the radar pulse.

GCC method finds the TDOA by selecting the time corresponding to the peak of correlation function of received signals. GCC method is applicable for Monopulse applications. Furthermore GCC is shown to be successful under indoor reverberation to some extent [3]. On the contrary performance of GCC is not known in the land multipath environment to the best of our knowledge.

In this thesis, a land based DF system with two spatially separated sensor sites measuring the TDOA between received radar signals is presented. The effects of multipath channel, system parameters and radar parameters on AOA estimation performance are investigated. Furthermore improving effects of diversity on AOA estimation performance is investigated. Lastly a realistic scenario is studied and AOA estimation performance of a realistic system is investigated.

1.2 Outline of the Thesis

The outline of the thesis is given below:

In Chapter 2 AOA estimation methods are discussed.

In Chapter 3 alternative TDOA estimation methods are discussed and system model used in this thesis is presented.

In Chapter 4 performance evaluation of the system proposed in Chapter 3 is done. Furthermore effects of channel, system and radar parameter on AOA estimation performance are investigated through Monte Carlo simulations.

Chapter 5 is about the improving effects of diversity on AOA estimation performance.

A realistic scenario for the proposed system is presented in Chapter 6.

Finally conclusions are drawn and some future work is proposed in Chapter 7.

CHAPTER 2

AOA ESTIMATION

AOA is the only parameter, which gives information about the location of a radar. Furthermore, it is the only parameter that the radar cannot change in a short time. This makes the estimation of AOA very important in EW receivers. The following assumptions are commonly used in solving AOA estimation problem, [7]:

- Radar is located at the far field of the receiver array
- Both the sensors in the array and the radar are in the same plane
- Radar is a point emitter.

Under these assumptions passive AOA estimation techniques for a radar signal can be divided into 2 categories:

1. Instantaneous (monopulse) AOA estimation techniques: AOA information is obtained by processing a single pulse of the radar.
2. Multipulse AOA estimation techniques: AOA information is obtained by processing a group of pulses of the radar.

Since it is dealt with instantaneous AOA estimation in this thesis, hereafter instantaneous AOA estimation techniques will be analyzed.

Instantaneous AOA estimation techniques can be categorized into 3 groups:

1. Amplitude comparison monopulse
2. Phase comparison (interferometer) method
3. TDOA method

Furthermore hybrid of Amplitude comparison and Phase Comparison method is also possible.

2.1 Amplitude Comparison Monopulse DF

A system, which uses amplitude comparison monopulse, finds the AOA of the incoming signal by comparing the amplitudes of the signals received by squinted antennas. A typical DF system, which uses Amplitude Comparison Monopulse, is given Figure 2-1. In order to have a 360° coverage, antennas can be located as given Figure 2-2.

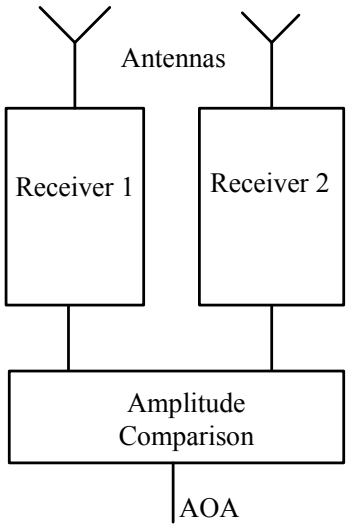

Figure 2-1: A typical DF system which uses amplitude comparison Monopulse DF

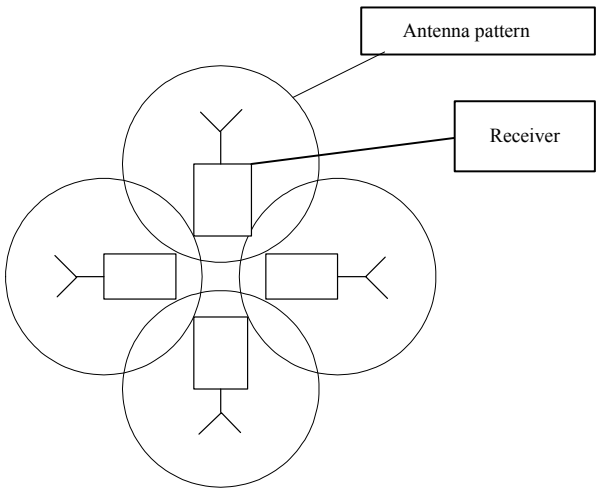

Figure 2-2: Location of antennas in a typical DF system which uses amplitude comparison Monopulse DF

In an amplitude comparison monopulse system, imbalance between the receiver channels is an important source of error for AOA estimation. Since the multipath environment causes random amplitude fluctuation on the received signals, amplitude comparison method is not suitable for multipath environment, [2].

2.2 Phase Comparison Monopulse DF

In a system, which uses phase comparison monopulse, AOA is estimated by using the phase difference of received signals, [2]. A typical DF system, which uses phase comparison monopulse, is given in Figure 2-3.

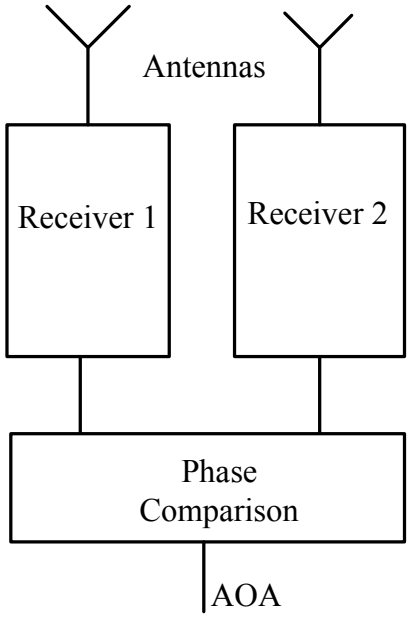

Figure 2-3: A typical DF system which uses phase comparison Monopulse DF

Let the received signal at two receivers be $r_1(t) = \sin(2\pi ft)$ and $r_2(t) = \sin\left(2\pi ft + \frac{2\pi d}{\lambda}\sin(\theta)\right)$ where d is the distance between sensors, λ is the wavelength of the received signal, f is the carrier frequency of the received signals and θ is the actual AOA of the received signal. The phase difference between the received signals, $\frac{2\pi d}{\lambda}\sin(\theta)$ is caused by the extra path, $l = d\sin\theta$ traveled by the signal arriving at the second sensor. If the phase difference between the received signals can be extracted, then the AOA information can be found by an inverse sine transformation.

2.3 DF with TDOA

AOA estimation with TDOA method finds the direction of arrival of a signal from the information of time difference of arrival of the signal at the sensors, [6]. General structure of a system that finds AOA with TDOA is given in Figure 2-4.

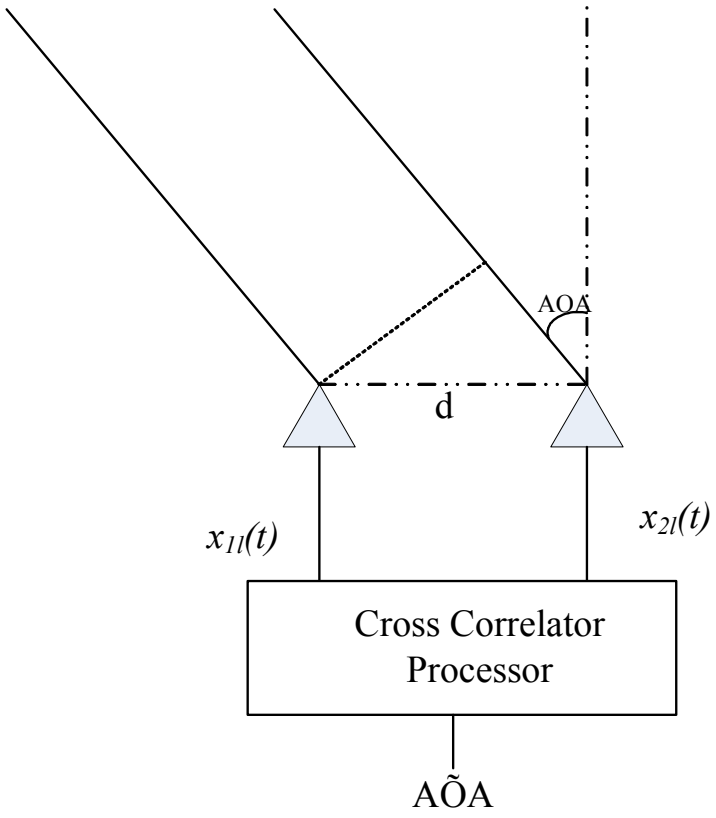

Figure 2-4: A typical DF system which uses TDOA

In the system shown in Figure 2-4, it is assumed that the distance of source to the sensor sites is much greater than the distance between sensor sites. This assumption is necessary for application of TDOA method in AOA estimation. Furthermore it is assumed that sensor sites are synchronized. Synchronization of the sensor sites may be achieved by utilization of GPS. Synchronization accuracy required for a TDOA system is derived in Appendix A.

Let the signals received by the two sensor sites 1 and 2 be $r_1(t) = s(t)$ and $r_2(t) = s(t - TDOA)$ respectively, where $s(t)$ is the radar pulse and $TDOA$ is the time difference of arrival between sensor sites. In this case AOA of the received

signal in Figure 2-4, can be written as $AOA = \arcsin(\frac{c * TDOA}{d})$ where d is the distance between sensor sites and c is the velocity of the light.

Since amplitude comparison monopulse and phase comparison monopulse techniques are known to fail in multipath environment [2], in order to investigate the performance of TDOA in multipath environment, TDOA is selected as AOA estimation method in this thesis.

CHAPTER 3

AOA ESTIMATION BY TDOA IN A MULTIPATH ENVIRONMENT

In this chapter AOA estimation by TDOA is discussed in detail. First TDOA estimation techniques in the literature are investigated. Then the optimum system structure for estimating AOA with TDOA is discussed. Lastly signal and system model used in this thesis is explained.

3.1 TDOA Estimation

Since AOA is related to TDOA by a sine transformation, accuracy of the AOA estimation by TDOA depends on TDOA estimation performance. Hence TDOA estimation techniques are investigated and a comparison is made according to their properties.

3.1.1 Generalized Crosscorrelation Method

GCC method finds the maximum value of cross correlation of prefiltered signals. A typical generalized crosscorrelation function for received signals $x_1(t) = s_1(t) + n_1(t)$ and $x_2(t) = s_1(t + D) + n_2(t)$ can be written as

$$\int_{-\infty}^{\infty} H_1(f)H_2^*(f)G_{x_1x_2}(f)e^{j2\pi f\tau}df \tag{3-1}$$

where $G_{x_1x_2}(f)$ is the cross power spectrum function of $x_1(t)$ and $x_2(t)$, $H_1(f)$ and $H_2(f)$ are the frequency domain prefilters of $x_1(t)$ and $x_2(t)$ respectively, $s_1(t)$ is emitted signal by the source and $n_1(t)$ and $n_2(t)$ are the additive white Gaussian noise. Then a weighting function can be defined as

$$\psi_g(f) = H_1(f)H_2^*(f) \tag{3-2}$$

In the literature weighting function is derived form the power spectra of the signals $x_1(t)$ and $x_2(t)$. The weighting functions in the literature are given in Table 3-1, [8].

Table 3-1: Weighting functions in the literature

Processor name	Weight
Roth Impulse response	$\frac{1}{G_{x_1x_2}(f)}$
SCOT	$\frac{1}{\sqrt{G_{x_1x_1}(f)G_{x_2x_2}(f)}}$
PHAT	$\frac{1}{\lvert G_{x_1x_2}(f)\rvert}$
Eckart	$\frac{G_{s_1s_1}}{G_{n_1n_1}(f)G_{n_2n_2}(f)}$

Since the weighting functions given in Table 3-1 require the knowledge of the power spectra the received signal they are not applicable for nonrandom signal

model. If the weighting function, $\psi_g(f)$ equals one in the frequency range of interest, then the name of method is CC method. CC method is applicable for nonrandom signal model. GCC method with weighting functions given in Table 3-1, is mostly used in acoustic applications such as SONAR and speech processing, [3], [9], [10]. There is a vast amount of study made on GCC in the literature. The studies made on GCC can be categorized as:

1. Analytical Performance Evaluation of GCC, [8], [11], [12]
2. Discrete implementation of GCC, [13], [14]
3. Performance of GCC in a Multipath Environment, [3], [15], [16], [17], [18].

3.1.1.1 Analytical Performance Evaluation

In the literature performance evaluation of GCC method is done by following methods:

1. CRLB analysis, [8], [12]
2. Gross Error analysis, [11], [15].

When the SNR is high CRLB is an ideal reference for performance evaluation. CRLB for GCC method in a single path environment with random signal model assumption is derived by Carter, [8].

Probability of gross error of GCC is derived by Ianiello, [8]. Probability of Gross Error is used as a performance criterion when the SNR is low.

3.1.1.2 Discrete Implementation of GCC

In practical systems GCC is implemented in discrete form. Discrete implementation of GCC is discussed by Boucher, [14]. Boucher showed that the discrete implementation of GCC has a biased estimation performance at low sampling rates. Furthermore Jacovitti derived the MSE expression for discrete implementation of CC and evaluated its performance, [15]. It was shown that the performance was

close to the CRLB at high SNR cases. In addition, Jacovitti showed that TDOA estimation by minimization of MSE expression (AMDF) outperforms the CC for random signal model.

3.1.1.3 Performance in Multipath Environment

Performance of GCC is affected by multipath environment. Performance of GCC in room reverberation (indoor multipath) is analyzed in [3]. Performance of GCC in a scattering medium such as underwater environment is analyzed by Prasad, [18]. Furthermore in [13] it is shown that the performance of GCC is independent of multipath until a degree of room reverberation. On the other hand there is not a specific study on effect of outdoor land multipath environment on the performance of GCC.

3.1.2 Leading Edge (LE) TDOA

Let the signals received by sensor sites be as shown in Figure 3-1. Time of Arrival (TOA) of the received pulses can be estimated by determining the time corresponding to the Leading Edge of the pulses. When the TOA's of received signals are estimated, TDOA of the signals can be calculated by subtracting the estimated TOA's. TDOA estimation by LE method can only be applied to pulsed signals, due the presence of a leading edge. In the literature TDOA estimation by LE estimation in a single path environment is considered by ratio test, [19] and adaptive thresholding, [20].

If the tap intervals of the channel are on the order of rise time of the pulse, the leading edge of the received pulse will be distorted in a multipath environment and the performance of LE TDOA method will be poor. In Figure 3-2 undistorted and distorted pulse are given for channel tap interval 10^{-7} sec. and rise time $1.5*10^{-7}$ sec respectively.

In [21], probability of gross error is given for TOA estimation by LE. According to [21] gross error occurs when the duration of the rising edge exceeds the expected rising edge time. For single path LE TDOA estimation, it is assumed that gross error probability found in [21] is very small. On the other hand in a multipath environment, due to the distortion in the leading edge of the pulse gross error is generally larger than fine error.

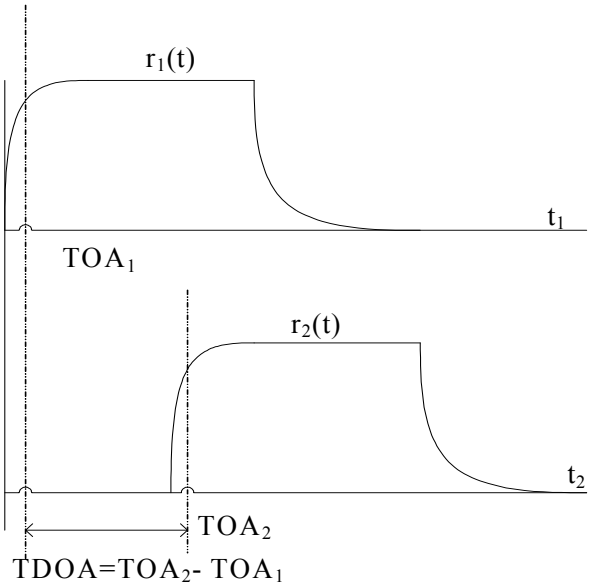

Figure 3-1: Received pulses for LE TDOA

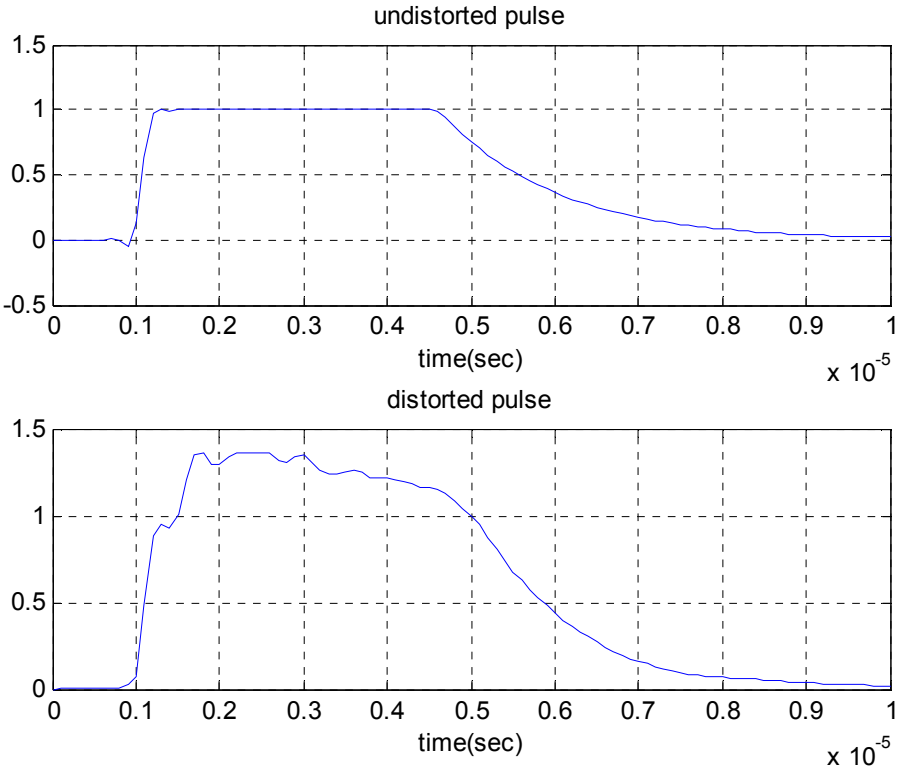

Figure 3-2: Undistorted and distorted pulses

3.1.3 Adaptive Algorithms for TDOA

If the emitter is moving, then the TDOA of the received signal varies with time. In order to track the time variation, adaptive TDOA algorithms are used. Reed used LMS for estimation of TDOA in a single path environment [4]. Furthermore in [5] it is shown that adaptive algorithms can also solve the TDOA estimation problem in multipath environment. On the other hand, due to the long convergence times of adaptive algorithms [5], they are not suitable for systems which find AOA from a single radar pulse.

3.2 Optimum Receiver Structure for TDOA Estimation

Optimum receiver structure for TDOA estimation is given in Figure 3-3. The receiver structure is optimum due to utilization of MAP estimator. Optimum receiver estimates the TOA's of the received signals and calculates the TDOA by subtracting the estimated TOA's from each other.

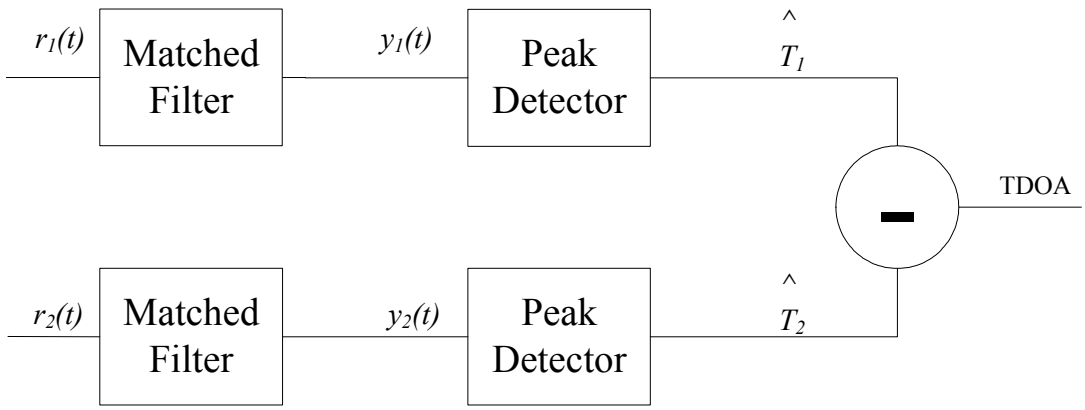

Figure 3-3: Optimum receiver structure for TDOA estimation

TOA estimation in the optimum receiver structure is well known in the literature, [22]. Let $s(t)$ be a pulse with arrival time A, and it is desired to find a "Maximum A Posteriori (MAP)" estimate of A.

In order to find the MAP estimate of A, it is known that the operation on the received waveform consists of finding the likelihood function as

$$\ln(\Lambda_1[r(t),A]) = \frac{2}{N_o}\int_{-T}^{T} r(u)s(u-A)du - \frac{1}{N_o}\int_{-T}^{T} s^2(u-A)du\,, \tag{3-3}$$

where $r(t)$ is the received waveform under white noise, which can be written as

$$r(t) = s(t) + w(t)\,. \tag{3-4}$$

The second term in (3-3) does not depend on A, since observation interval [-T, T] is assumed to contain entire pulse. The first term in (3-3) is a convolution operation, and the result of this convolution operation is equivalent to the output of a linear time invariant filter, $y(t)$ with impulse response $h(t)$ and input $r(t)$ over [-T, T].

$$y(t) = \int_{-T}^{T} r(u)h(t-u)du \tag{3-5}$$

If we let $h(t) = s(-t)$, then $h(t)$ is a matched filter. Time which corresponds to the peak of the matched filter is MAP estimate of TOA.

This receiver structure requires a priori information of the received signal waveform. If the received signal model is a non-random signal model, optimum receiver structure is not applicable.

3.3 System and Signal Model

System and signal model used in this thesis is discussed in this section. We consider 2 sensor sites followed by a crosscorrelator processor as shown in Figure 3-4.

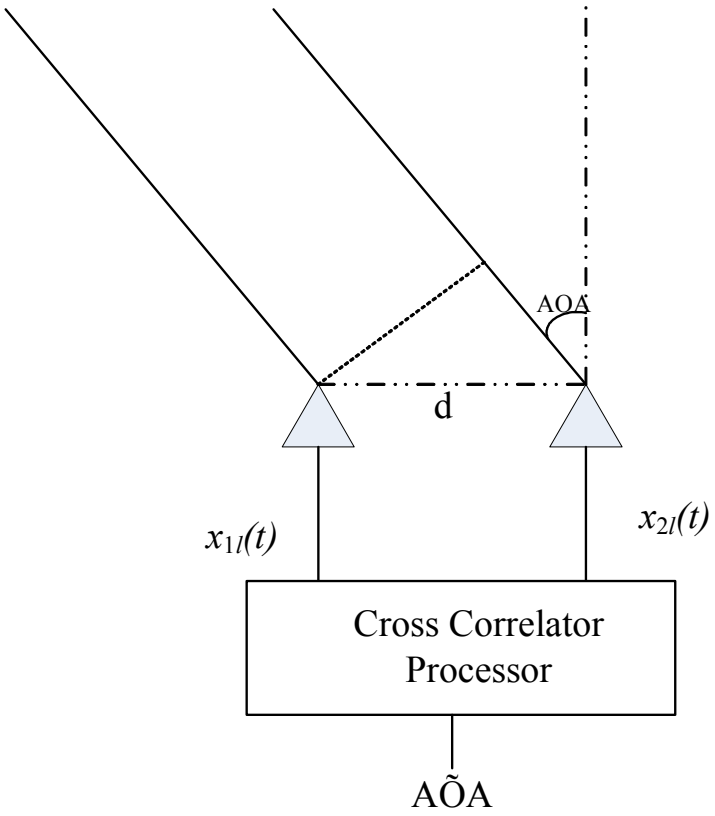

Figure 3-4: System model

Assuming that carrier frequency of the received signal is known, baseband model of each sensor site is given in Figure 3-5.

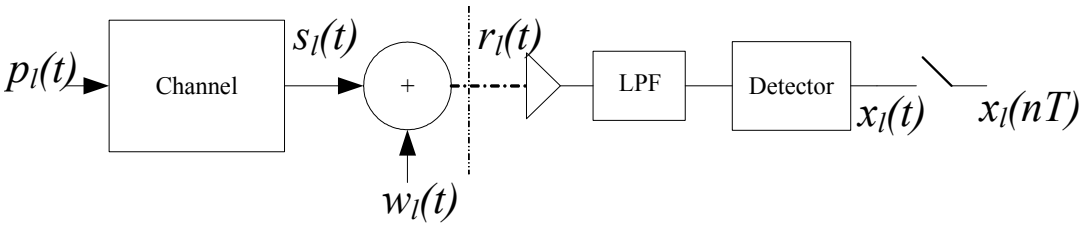

Figure 3-5: Baseband model of a sensor site

3.3.1 Emitted Signal by the Source

Emitted signal by the source is taken as a nonrandom radar signal in thesis. General form of a radar signal can be written as

$$p(t) = A(t)\cos\left(2\pi f_c t + \beta(t)\right) \tag{3-6}$$

where $A(t)$ is the envelope, $\beta(t)$ is phase modulation function and f_c is the carrier frequency of the radar signal. $A(t)$ is assumed to be a rectangular signal with a rise time, t_r, and a fall time, t_f. If there is no phase modulation in the radar pulse $\beta(t)$ is just a constant value.

Complex low pass equivalent of the radar signal, $p(t)$, can be written as

$$p_l(t) = A(t)\, e^{j\beta(t)} \tag{3-7}$$

where $e^{j\beta(t)}$ represents the phase of the signal. Since it is assumed that the carrier frequency of the radar signal is estimated accurately, complex low pass equivalent of the radar signal is used as emitted signal in this thesis.

3.3.2 Channel Structure

A realistic channel structure is used in this thesis. In order to explain the channel structure first LTV channel model is discussed, then how the LTV channel is simplified to LTI channel is shown.

3.3.2.1 LTV Channel

Complex valued lowpass transfer function of LTV channel can be written as $c(\tau, t)$ where τ represents path delay and t accounts for the time variation of the channel. $c(\tau, t)$ is a complex Gaussian process in the t variable, [23].

First order statistical properties of the channel are defined by 2 functions of the channel transfer function:

1. Power Delay Profile
2. Doppler Profile

3.3.2.1.1 Power Delay Profile

Power delay profile of the channel, $\phi_c(\tau)$, is the average power output of the channel, [23]. Mathematical expression for $\phi_c(\tau)$ with WSSUS assumption is given below:

$$\phi_c(\tau) = \frac{1}{2} E\left\{c^*(\upsilon+\tau,t)c(\upsilon,t)\right\} \tag{3-8}$$

The range of values of τ over which $\phi_c(\tau)$ is nonzero is called delayspread of the channel. Average power delay profiles according to Cost 207 are given below, [24]:

a. Typical case for rural (non-hilly) area;

$$\phi_c(\tau) = \begin{cases} e^{-9.2\tau} & 0 \le \tau \le 0.7\,\mu\text{sec} \\ 0 & \text{else} \end{cases}$$

b. Typical case for urban (non-hilly) area;

$$\phi_c(\tau) = \begin{cases} e^{-\tau} & 0 \le \tau \le 7\,\mu\text{sec} \\ 0 & \text{else} \end{cases}$$

c. Typical case for hilly urban area;

$$\phi_c(\tau) = \begin{cases} e^{-\tau} \text{ for} & 0 \le \tau \le 5\,\mu\text{sec} \\ e^{5-\tau} \text{ for} & 5 \le \tau \le 10\,\mu\text{sec} \\ 0 & \text{else} \end{cases}$$

d. Typical case for hilly terrain;

$$\phi_c(\tau) = \begin{cases} e^{-3.5\tau} \text{ for} & 0 \le \tau \le 2\,\mu s \\ 0.1e^{15-\tau} \text{ for} & 15 \le \tau \le 20\,\mu s \\ 0 & \text{else} \end{cases}$$

3.3.2.1.2 Doppler Profile

Doppler profile is a function of channel transfer function which determines the time variations of the channel, [23]. Mathematical expression for Doppler profile is given below:

$$S_c(\lambda) = \int_{-\infty}^{\infty} \phi_c(\Delta t) e^{-j2\pi\lambda\Delta t} d\Delta t \tag{3-9}$$

The range of values for which Doppler profile of the channel is nonzero is called Doppler spread, $B_{d,}$ of the channel. Reciprocal of B_d is called coherence time of the channel. Coherence time of the channel is a statistical measure of the time duration over which the channel impulse response is invariant. A slowly varying channel has a long coherence time.

3.3.2.2 LTI Channel Structure

Since the direction finding system defined in this thesis finds the AOA from a single radar pulse, the observation time used by the receiver are assumed to be small compared to the coherence time of the channel. Hence the channel is assumed to be LTI during the observation time of the system.

3.3.2.3 Physical Description of the Channel

Channel model depends on the physical propagation environment of the waves. Terrain over which the waves propagate affects the following parameters of the channel:

- Shape of average power delay profile.
- Delay spread
- Ratio of the power of line-of-sight (LOS) signal to the total power of scattered signals.

According to the Cost 207 report physical outdoor land environments for the multipath channel can be categorized as follows, [24]:

- Urban environment

An urban area describes a typical, heavily built up, down town area within city. Tall buildings along streets act as reflector of radio waves and a line-of-sight (LOS) does not exist because of shadowing of nearby buildings.

- Hilly urban environment

If the city is in a mountainous region then there may be strong reflections with large delays from the far away mountains. Since the area is heavily built up average power delay profile is modeled by 2 exponentials following each other.

- Rural environment

Rural area describes the less built up outskirts of the city. Rural areas are usually open environments. LOS signal occurs with higher probability compared to urban area due to less shadowing.

- Hilly terrain environment

If the rural area is in a hilly environment such as a valley, then there may be strong reflections with large delays from far away mountains. In hilly terrain area since the region between far away reflector and nearby reflectors is open area average power delay profile is modeled by discrete exponential functions.

3.3.3 Noise Process

Noise process used in the system, $w_l(t)$ is assumed to be additive complex white Gaussian process. Its lowpass model is used in the system model.

3.3.4 Receiver Structure

Receiver used in the system is composed of following components:

a) Sensor

Sensors are assumed to be omnidirectional for simplicity. On the other hand, when the sensors are omnidirectional delay spread of the channel increases at the same time. When the sensors are omnidirectional, the system receives the reflections of emitted signal from all of the directions. This increases the delay spread. But when the sensors are directive, the system receives the reflection from a limited angular coverage, [25].

b) LPF

LPF represents the IF and RF filters in the receiver. Since EW systems aim to cover a large bandwidth, BW of RF filters in the front end are much greater than the BW of the IF filter. Thus BW of the LPF is taken as BW of IF filter, [6]. Furthermore, since pulsewidth of the received radar pulse is not known BW of the LPF is chosen according to expected minimum pulsewidth radar pulse.

c) Envelope detector

In order to extract the envelope of the received signals an envelope detector is used. Since the incoming signal is not known, phase of the channel coefficients cannot be estimated. Hence a noncoherent detector is used after the IF filter structure. Coherent receiver structure is only possible when the incoming signal is known. Mathematical expression for the detector is $|\ |^n$, where n is the order of the detector. "n" will be used as a design parameter in the system model. Its effect on estimation performance will be explained in section 5.3.4.2.

d) A/D Converter

Since the BW of the received signals is limited to the BW of IF filter in the receiver, the sampling rate of the A/D is twice the BW of the IF filter of the receiver. The resolution of the TDOA estimation is mainly determined by sampling rate of the A/D. Hence sampling rate of the receiver affects the estimation performance directly.

3.3.5 Processor Model

As a result of the comparisons of TDOA estimation techniques made in section 3.1, cross correlation method is determined as the most suitable one due to the following reasons:

- Crosscorrelation is applicable for monopulse TDOA estimation
- Performance of Crosscorrelation is independent of multipath until a degree of delay spread, [3].

Let the received signals be

$$r_{l1}(t) = \int h_1(\tau) p_l(t-\tau) d\tau + w_{l1}(t) \tag{3-10}$$

$$r_{l2}(t) = \int h_2(\tau) p_l(t - TDOA - \tau) d\tau + w_{l2}(t) \tag{3-11}$$

where $h_1()$ and $h_2()$ are channel transfer functions and $w_{l1}()$ and $w_{l2}()$ are zero mean additive white Gaussian noise processes.

The signals after the envelope detector and A/D are given below:

$$x_{l1}(nT) = |r_{l1}(nT)|^n \tag{3-12}$$

$$x_{l2}(nT) = |r_{l2}(nT)|^n \tag{3-13}$$

After the A/D, received signals are fed into the crosscorrelator processor. The mathematical expression for cross correlation function is given below:

$$R(\tau) = \frac{1}{N} \sum_{n=1}^{N} x_{l1}(nT) x_{l2}(nT + \tau) \tag{3-14}$$

After the cross correlation function is calculated, peak of the cross correlation function is determined. Delay which corresponds to the peak is TDOA between the received signals.

In order to estimate the noninteger multiples of the sampling interval, interpolation has to be applied to the cross correlation function. Since samples around the peak of the crosscorrelation function can be approximated by a parabola, parabolic interpolation can be applied to the cross correlation function. Expression for the TDOA estimate after parabolic interpolation is given below.

$$TDOA = T_{TDOA} + \frac{1}{2}\left(\frac{R(T_{TDOA} + T) - R(T_{TDOA} - T)}{2R(T_{TDOA}) - R(T_{TDOA} + T) - R(T_{TDOA} - T)} \right) \qquad (3\text{-}15)$$

where T_{TDOA} is time difference of arrival estimated before interpolation and $TDOA$ is time difference of arrival estimated after interpolation. Since parabolic interpolation uses three samples of the crosscorrelation function it is computationally efficient. On the other parabolic interpolation introduce a bias to the estimation at low sampling rates, [14].

After the $TDOA$ is estimated, AOA is found by the following formula:

$$AOA = \sin^{-1}\left(\frac{TDOA * c}{d} \right) \qquad (3\text{-}16)$$

CHAPTER 4

PERFORMANCE OF AOA ESTIMATION WITH TDOA

In this chapter performance of AOA estimation with crosscorrelation TDOA method is evaluated through Monte Carlo simulations. In order to evaluate the performance of the method, following are done:

1. Performance evaluation criterion is defined
2. Simulation methodology is defined
3. Monte Carlo simulations are run

4.1 Performance Evaluation Criterion

Performance evaluation criterion used in this thesis is the RMS error. RMS error is composed of fine errors and gross errors. When the RMS error is composed of fine errors, it is reasonable to compare RMS error with a performance bound such as CRLB. Derivation of the CRLB depends on the signal model. In the literature there are various CRLBs derived for various signal models, [8], [12]. For the signal model described in section 3.3.1 and under single path channel model assumption, CRLB for AOA estimation with TDOA method (equation (4-1)) is derived. Detailed derivation of the CRLB is given in Appendix B.

$$CRLB(AOA) = \frac{\frac{N_o T_s}{4A}}{\left(\frac{d}{c}\right)^2 - (TDOA)^2} \tag{4-1}$$

On the other hand when the gross errors dominate the rms error, using a performance bound is meaningless, [22]. Gross errors dominate the RMS error in 2 cases given below:

1. When the SNR is low, [11]
2. When the propagation environment of the received signal is multipath, [3], [15]

In the literature probability of gross error is used in order to evaluate the performance when the gross error dominates the RMS error, [3], [11], [15]. In this thesis definition for probability of gross error is as follows:

Let θ_{lim} be the maximum AOA RMS error for the system. The ratio of the number of Monte Carlo trials in which the error is above θ_{lim} to the number of total trials is called the probability of gross error.

In order to derive the θ_{lim}, first maximum TDOA rms error, $TDOA_{lim}$, must be known. In the literature $TDOA_{lim}$ is taken as half of the correlation time of the signal, [11]. Correlation time is the duration which the autocorrelation function of the received signal is nonzero. For a pulsed signal, correlation time is on the order of the pulsewidth. Since pulsewidth of the received signal is much larger than the sampling period, it is not reasonable to take $TDOA_{lim}$ equal to correlation time. One reasonable approach for choosing $TDOA_{lim,}$ is equating it to the time between first and second tap. Since there is a nonlinear relationship between $TDOA_{lim}$ *and* θ_{lim}, θ_{lim} is chosen arbitrarily in this thesis.

As a final remark, although gross error probability is used as performance criterion, gross errors are included in RMS error and standard deviation values.

4.2 Simulation Methodology

Simulation methodology used in this thesis is explained in this section. First the implementation of the system model given in section 3.3 in Matlab is discussed, then how the Monte Carlo simulations are done is explained.

4.2.1 Implementation of the System in Matlab

System model given in section 3.3 is implemented as given in Figure 4-1

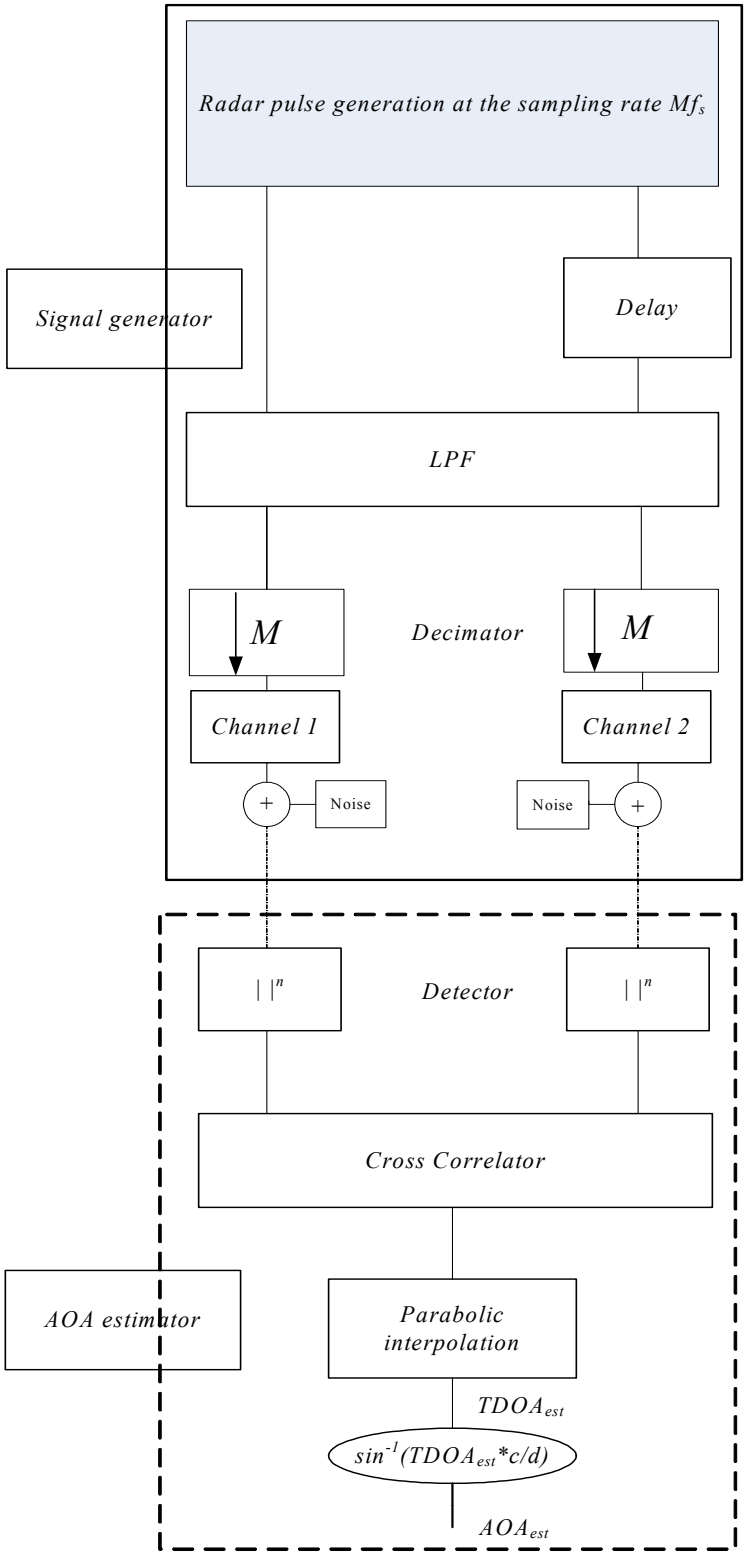

Figure 4-1: Implementation of system model in Matlab

System model given in Figure 4-1 has 2 subsystems:

1. Incoming signal generator
2. AOA estimator

AOA estimator's implementation is no different than the one explained in section 3.3.5, hence only implementation of incoming signal generator is discussed here.

4.2.1.1 Incoming Signal Generator

Incoming signal generator generates the signal at the sensors. Its operation is composed of 3 phases:

1. Radar pulse generation
2. Channel modeling
3. Noise addition

4.2.1.1.1 Radar Pulse Generation

The signal shape for pulsed radars is generally a rectangular pulse with a steep rising edge, thus it has a large bandwidth in the order of the reciprocal of rise time. In practical systems the analog radar pulse is first passed through IF filters and then sampled. In the simulations since it is not possible to generate radar pulse in analog form, it is generated in discrete form. When the pulse is generated at the Nyquist rate corresponding to the IF bandwidth of the receiver, effects of low pass filtering on the rising edge of the pulse cannot be seen. In order to solve this problem radar pulse is generated at a much higher sampling rate, passed through a lowpass filter and then decimated to the desired sampling rate. Procedure described above is summarized in Figure 4-20, [6].

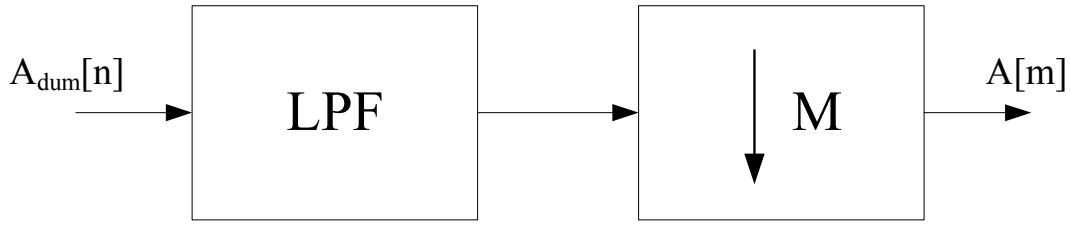

Figure 4-2: Block diagram for radar pulse generation

Implementation details of components in Figure 4-2 are given below:

- LPF

As described in section 3.3.2 in order to model the IF filter in the system a LPF is used. LPF used in the simulations is an FIR filter. FIR filter is obtained by sampling of a raised cosine filter with sampling period T=1/*$M f_s$ where M is the decimation rate. Rectangular filter is not used because the sharp edges of rectangular filter cause ripples on the generated pulse. The impulse response of a raised cosine filter is

$$h_{LPF} = \sin(2B_T t)\frac{\cos(2\pi\rho B_T t)}{1-16\rho^2 B_T^2 t^2} \tag{4-2}$$

where ρ is the roll-off factor and B_T is the symmetry frequency of the filter.

Furthermore bandwidth of the LPF filter used in the simulations is equal to the half of the desired sampling frequency, f_s.

- Decimator

After the pulse is generated at a high sampling rate, f_h and passed through a LPF, it is still in an oversampled form. In order to decimate its sampling rate to desired sampling rate, decimator decimates the output of the LPF by a factor $M = f_h / f_s$.

4.2.1.1.2 Channel Modeling

Generated radar pulses are passed through a realistic channel. Realistic Channel is modeled by a tapped delay line as shown in Figure 4-3, [23]. For a NLOS tap

coefficients $a_0, a_1, \ldots a_k$ are independent zero mean complex Gaussian random variables. On the other hand, if the channel is LOS, a_0 has a nonzero mean. It is assumed that $E\{a_0^2\} + E\{a_1^2\} + \ldots + E\{a_k^2\} = 1$, so that the channel does not give a gain to the emitted signal, [26]. In order to define the amount of LOS signal in a channel parameter given below is defined, [27].

$$K = \frac{power\ \ of\ \ LOS\ \ signal}{total\ \ power\ \ of\ \ scattered\ \ signals} = \frac{E\{a_0^2\}}{\sum_{i=2}^{k} E\{a_i^2\}} \tag{4-3}$$

Tap spacing T is proportional to the inverse of IF bandwidth (BW) of the receiver and is equal to the sampling period of the receiver.

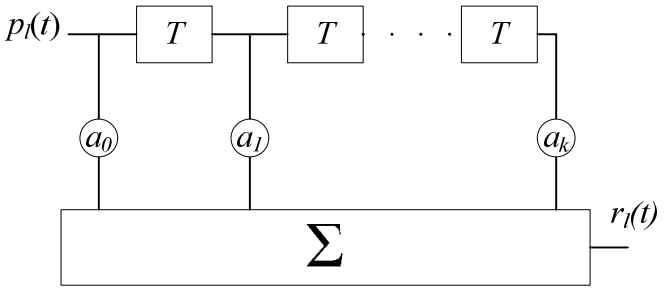

Figure 4-3: Tapped delay line

Delay spread of the channel is defined as kT, where k is proportional to the number of taps. If k=0 then the channel is single path, else multipath. Doppler spread of the channel is assumed to be zero, since the coherence time of the channel is assumed to be much greater than the observation time, [23].

According to the channel model given above, the noiseless received signal can be written as

$$r_{l1}(t) = \sum_{i=0}^{k} a_i p_l(t - iT) \tag{4-4}$$

4.2.1.1.3 Noise Addition

After the generated pulses are passed through the channel, additive white Gaussian noise is added to the channel output. Since the radar pulses are first generated at a high sampling rate then lowpass filtered, noise must go through the same operations. On the other hand since noise is generated in each run of Monte Carlo simulation, applying the LPF filtering to the noise increases the computational burden. In order to solve this problem noise is generated at the desired sampling rate and low pass filtering is not applied.

Amount of noise added to the channel output is determined according to the energy SNR. Expression for the Energy SNR is as follows:

$$SNR_e = \frac{E_{rp}}{N_o} \tag{4-5}$$

where E_{rp} is the energy of the radar pulse and N_o is the single sided spectral height of the noise.

Energy of the noiseless received signal can be written as

$$\int_0^{T_{obs}} E\left\{\left(\sum_{i=0}^{k} a_i p_l(t-iT)\right)\left(\sum_{i=0}^{k} a_i p_l(t-iT)\right)^*\right\}dt \tag{4-6}$$

In the above expression cross terms are equal to zero since the tap coefficients, $a_0, a_1, \ldots a_k$ are uncorrelated. Then the expression above is equal to

$$\int_0^{T_{obs}} E\left\{\left(\sum_{i=0}^{k} |a_i|^2 p_l^2(t-iT)\right)\right\}dt = \underbrace{E\left(\sum_{i=0}^{k} |a_i|^2\right)}_{1}\underbrace{\int_0^{T_{obs}} p_l^2(t-iT)dt}_{E_{rp}} = E_{rp} \tag{4-7}$$

Since $E\{a_0^2\}+E\{a_1^2\}+\ldots+E\{a_k^2\}=1$, the energy of the received signal is equal to the energy of the radar pulse generated at the source.

4.2.2 Monte Carlo Simulations

After describing the implementation of the system model in Matlab, general procedure of the Monte Carlo simulations carried out is explained in this section. General procedure for the Monte Carlo simulations is given below:

1. Set the following radar parameters:
    a. Radar pulse width
    b. Radar pulse AOA
    c. Pulse Type
2. Set the following Channel Parameters
    a. Channel average power delay profile type
    b. Channel delay spread
    c. *K* (Ratio of power of LOS signal to the total power of scattered signals)
3. Set the following system parameters
    a. Distance between sensors
    b. Sampling Rate
    c. SNR
4. Generate a radar pulse according to given parameters in step 1
5. Find the required TDOA according to the AOA given in step 1
6. Delay the radar pulse generated in step 4 and obtain the second pulse required for the TDOA estimation
7. Generate channel 1 and channel 2 according to the given parameters in step 2.
8. Pass the radar pulse 1 and pulse 2 through channel 1 and channel 2 respectively.
9. Add noise according to the given SNR.
10. Crosscorrelate the obtained signals in step 9.

11. Find the time corresponding to the peak of the correlation function and apply the parabolic interpolation.
12. Find the TDOA and convert it into AOA information
13. Repeat steps 7 to 12 for desired number of trials
14. Obtain RMS error, standard deviation and mean values according to the method given in Appendix C.

4.3 Simulation Results

While carrying out Monte Carlo simulations, effects of variation in simulation parameters on the estimation performance are observed. Simulation parameters which affect the AOA estimator performance can be categorized into three groups:

1. System Parameters
2. Channel Parameters
3. Radar Parameters

4.3.1 Effect of System Parameters

System parameters, which affect the estimation performance, are given below:

1. Observation window length
2. IF filter bandwidth
3. Distance between sensor sites
4. Type of crosscorrelator

4.3.1.1 Effect of Observation Window Length

Observation window length is the time in which the receivers observe the channel in order to receive the signal. For a nonrandom radar signal model, since the received signal is pulsed, it is important to capture the radar pulse during the observation window length. Hence it can be determined that minimum observation time is

$$observation\ window\ length = \frac{d}{c} + T_p$$

where d is the distance between sensors, c is the speed of light and T_p is the expected radar pulsewidth. On the other hand, when observation window length is increased, amount of noise in observation window is also increased.

In order to show the effect of observation window length to estimation performance Monte Carlo simulation with parameters given in Table 4-1 is carried out.

Table 4-1: Simulation parameters for observing effects of observation window length

Source signal	A rectangular radar pulse of pulse width 4.5μsec
Average power delay profile	Exponential power delay profile $e^{-t/\tau_\epsilon}u(t)$
Delay spread	2 μsec
Observation time	Changed from 4 μsec to 1000 μsec
Doppler spread	Ignored
Signal AOA	60°
SNR	Changed from 10 dB to 60 dB
Distance between sensor sites	750 m
Sampling rate	10 MHz
BW of LPF	5 MHz
Number of runs	4000
n	2
K	0
Θ_{lim}	2°

On Figure 4-4 and Figure 4-6 AOA RMS error and gross error probability are given as a function of observation window length for an SNR of 60 dB. It can be seen that RMS error is very large at 4 μsec. This is because radar pulse in the second sensor

site is not observed completely during the observation time. Furthermore it is observed that the effect of the increase in the observation window length to the estimation performance is not visible at high SNRs.

On the other hand when SNR is 30 dB the plots shown in Figure 4-5 and Figure 4-7 are obtained. On the figures it can be seen that AOA RMS error and gross error probability increases with increasing observation window length.

Hence it can be deduced that increasing observation window length above its minimum value degrades the performance when SNR is low. Since DF systems work on high SNR environments, it can be concluded that observation window length can be chosen as large as possible, provided that it is smaller than coherence time of the channel and SNR is high enough.

As a last remark since distribution of the AOA estimates for small observation window lengths is not Gaussian, confidence interval are not plotted for small confidence intervals.

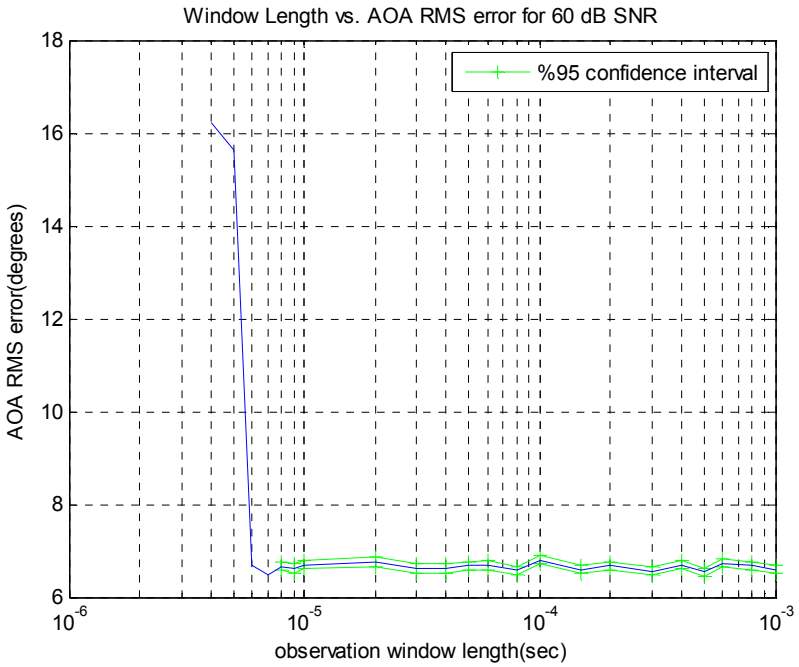

Figure 4-4: Observation window length versus AOA RMS error for 60 dB SNR

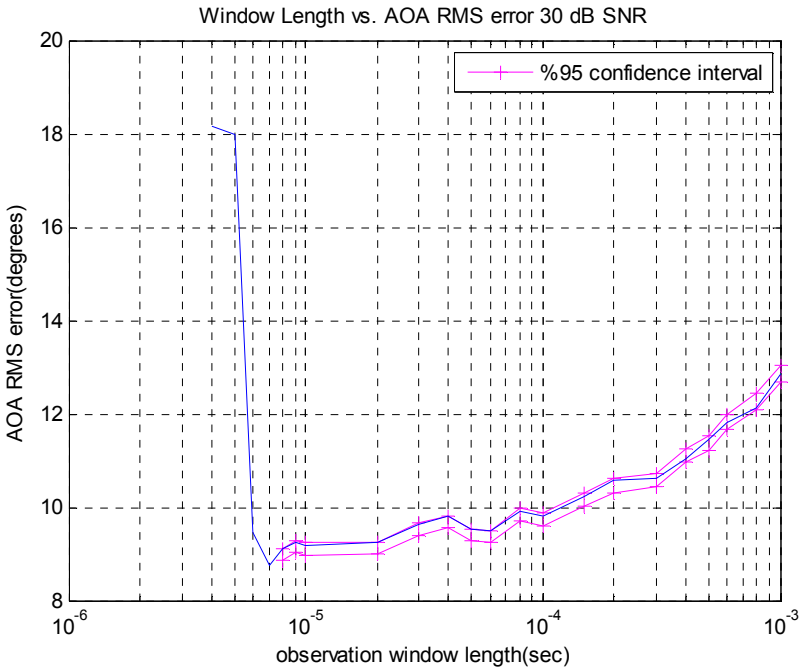

Figure 4-5: Observation window length versus AOA RMS error for 30 dB SNR

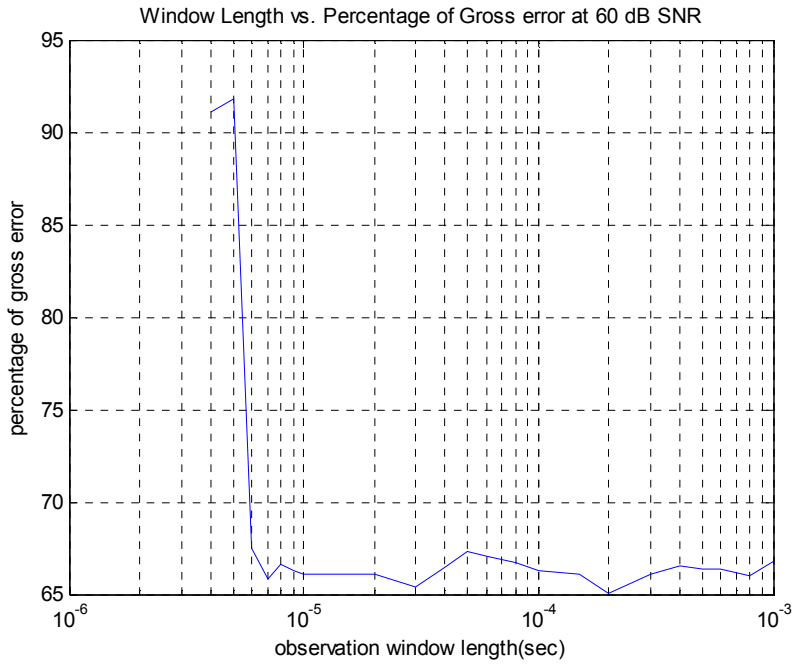

Figure 4-6: Observation window length versus Percentage of Gross Error for 60 dB SNR

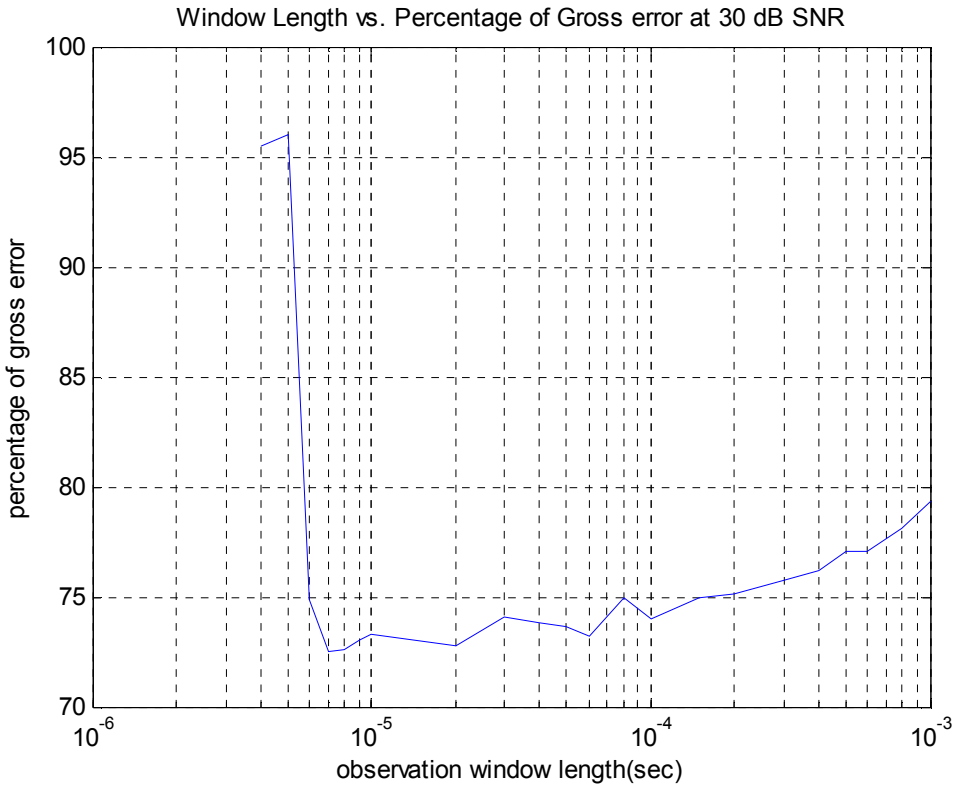

Figure 4-7: Observation window length versus Percentage of Gross Error for 30 dB SNR

4.3.1.2 Effect of IF Filter Bandwidth

Since sampling rate of the receiver is equal to twice the IF BW of the receiver , IF BW determines the time resolution of the system. Then an increase in the IF BW also increases the time resolution of the system. On the other hand, since the tap intervals of the channel model given in section 3.3.2 are equal to the inverse of the IF BW, IF BW also affects the complexity of the channel. Furthermore when IF BW is increased, power of the noise received by the system also increases. Thus change of the IF BW has both advantages and disadvantages.

In order to show the effect of IF BW on the estimation performance Monte Carlo simulations with parameters given in Table 4-2 are carried out.

Table 4-2: Simulation parameters for observing effects of IF filter bandwidth

Source signal	A rectangular radar pulse of pulse width 4.5μsec
Average power delay profile	Exponential power delay profile $e^{-t/\tau_c}u(t)$
Delay spread	2 μsec
Observation time	15 μsec
Doppler spread	Ignored
Signal AOA	60°
SNR	Changed from 10 dB to 60 dB
Distance between sensor sites	750 m
Sampling rate	Changed from 2 MHz to 200 MHz
BW of LPF	Changed from 1 MHz to 100 MHz
Number of runs	4000
n	2
K	0
Θ_{lim}	2°

On Figure 4-8 and Figure 4-10 AOA RMS error and Percentage of Gross Error are given as a function of IF bandwidth for a 60 dB SNR. On the figure it can be seen that increasing the IF BW after 10 MHz, does not have a visible effect on AOA estimation performance for high SNR case.

On the other hand when the SNR is 40 dB the plots given in Figure 4-9 and Figure 4-11 are obtained. It can be observed that the curve on the figure has a concave shape. Hence increasing the IF BW makes the AOA estimation performance worse for low SNR cases. This is expected, since the increase in the IF BW increases both the complexity of the channel and the noise power. Hence it can be said that improving effect of increase in the time resolution is cancelled by the increase in the

complexity of the channel and noise power for low SNR cases. But for high SNR cases since the noise power is too small, increasing IF BW does not decrease the SNR.

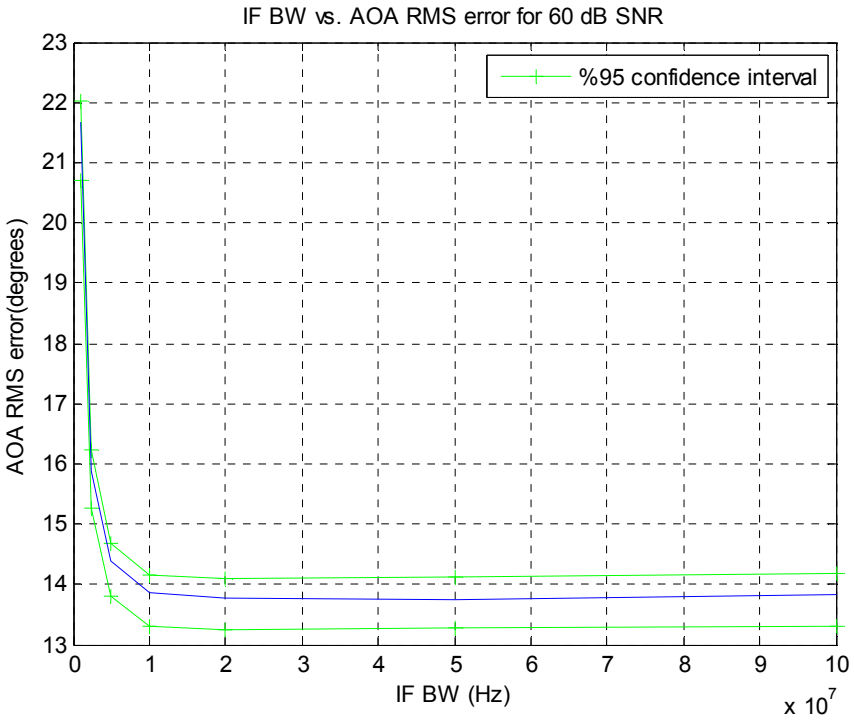

Figure 4-8: IF BW versus AOA RMS Error for 60 dB SNR

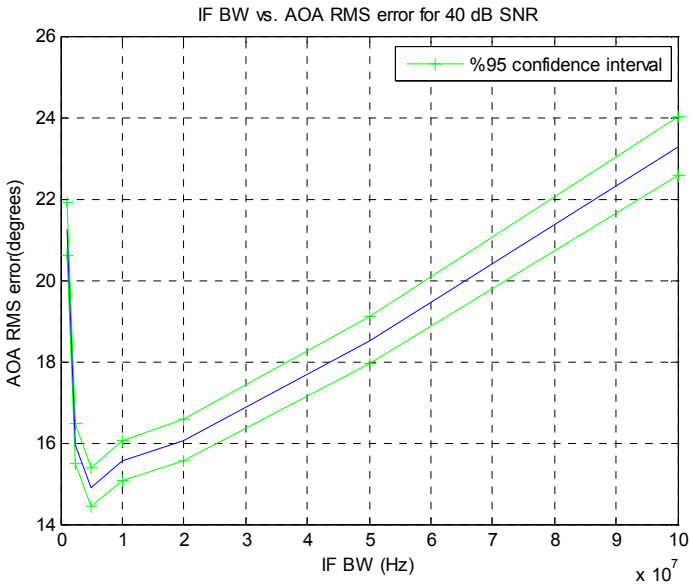

Figure 4-9: IF BW versus AOA RMS Error for 40 dB SNR

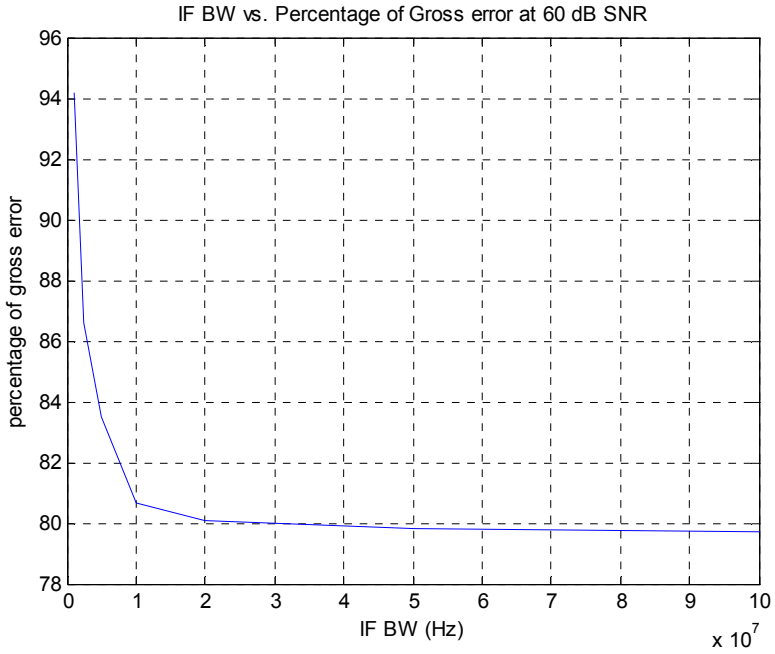

Figure 4-10: IF BW versus Percentage of Gross Error for 60 dB SNR

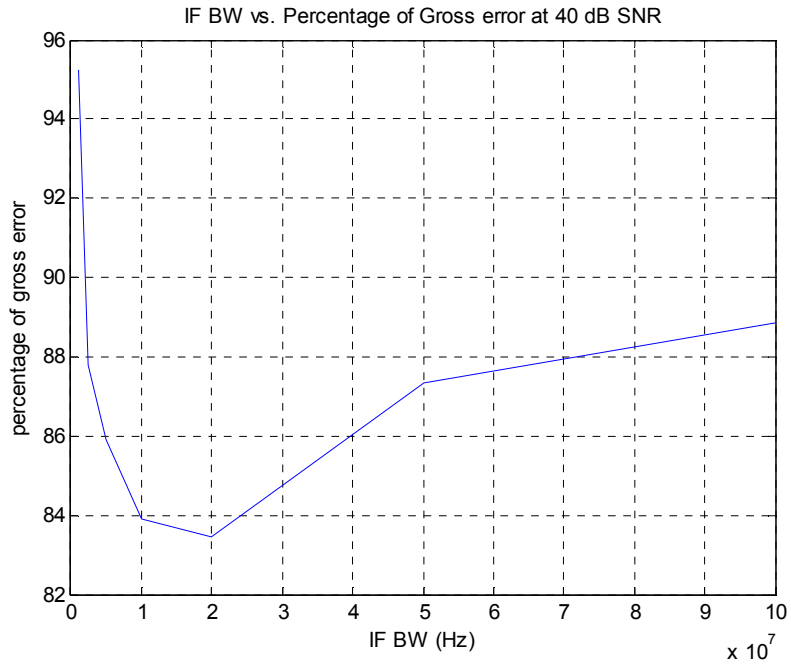

Figure 4-11: IF BW versus Percentage of Gross Error for 40 dB SNR

4.3.1.3 Effect of Distance between Sensor Sites

As given in section 3.3.5, after TDOA is estimated, AOA is found by the formula (3-16). As seen on the formula distance between sensor sites, *d*, directly affects the system performance provided that the sensor sites are fully synchronized. On formula (3-16) it can be noted that distance between sensor sites affects the resolution of the AOA. In order to show the effect of the distance between sensor sites on the AOA estimation performance, Monte Carlo simulations with parameters given in Table 4-3 are carried out.

Table 4-3: Simulation parameters for observing effect of distance between sensor sites.

Source signal	A rectangular radar pulse of pulse width 4.5μsec
Average power delay profile	Exponential power delay profile $e^{-t/\tau_c}u(t)$
Delay spread	2 μsec
Observation time	20 μsec
Doppler spread	Ignored
Signal AOA	60°
SNR	Changed from 10 dB to 60 dB
Distance between sensor sites	Changed from 500m to 3000 m
Sampling rate	10 MHz
BW of LPF	5 MHz
Number of runs	4000
n	2
K	0
Θ_{lim}	2°

On Figure 4-12 and Figure 4-13 AOA RMS error and percentage of gross error are given as a function of distance between sensor sites for constant energy SNR of 60 dB. As seen on the figures, as the distance between sensor sites increases, the AOA RMS error and gross error decreases. Although increasing of the baseline improves the performance, when the baseline and distance of emitters become comparable far field assumption given in chapter 2 is violated. Moreover minimum distance from the DF system in which a target has to be located increase, when the baseline increases. This decreases the detection probability of the target.

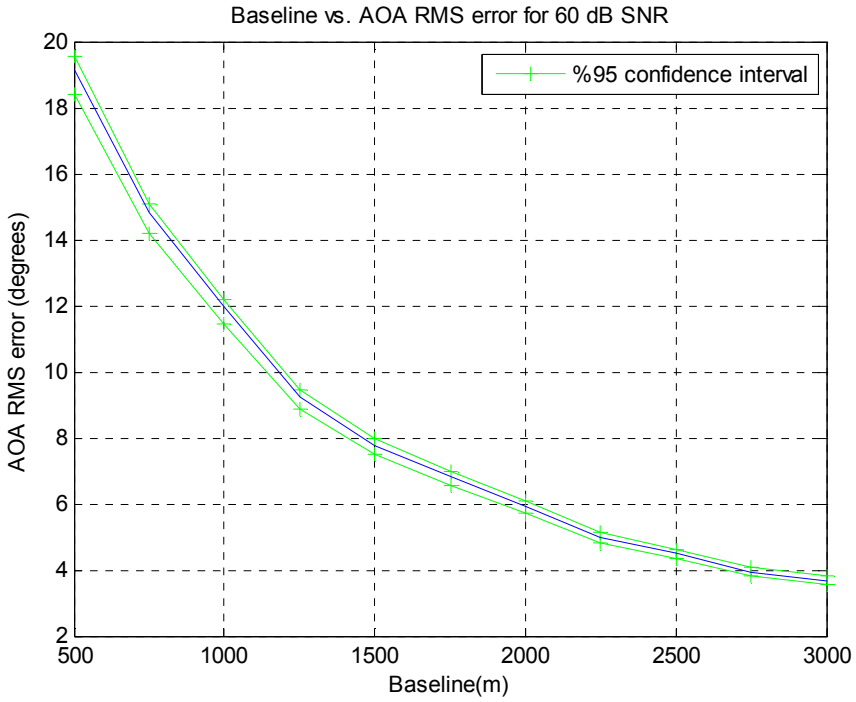

Figure 4-12: Baseline versus AOA RMS error at 60 dB SNR

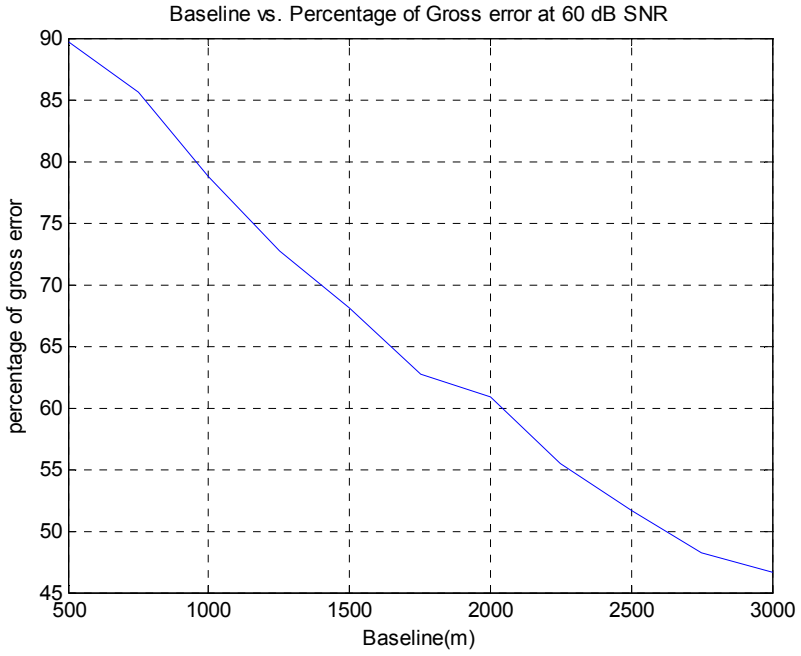

Figure 4-13: Baseline versus Percentage of Gross error at 60 dB SNR

4.3.1.4 Effect of Crosscorrelator Type

Since the signal received by the receiver is complex, TDOA of the received signals can be found by crosscorrelating either the complex signals directly or the envelope of the received signals. Hence there are two types of crosscorrelation that can be used, namely:

1. envelope crosscorrelation
2. complex crosscorrelation

Since the phases of the channel taps are not known, random phase of the channel taps distorts the crosscorrelation function. On the other hand in the case of envelope correlation, since the envelopes of the received signals are used, random phases of the channel taps do not affect the crosscorrelation function. In order to show the effect of the crosscorrelator type on the AOA estimation performance, Monte Carlo simulations with parameters given in Table 4-4 are carried out.

Table 4-4: Simulation parameters for observing effect of crosscorrelator type

Source signal	A rectangular radar pulse of pulse width 4.5μsec
Average power delay profile	Exponential power delay profile $e^{-t/\tau_e}u(t)$
Delay spread	2 μsec
Observation time	15 μsec
Doppler spread	Ignored
Signal AOA	60°
SNR	Changed from 10 dB to 60 dB
Distance between sensor sites	750 m
Sampling rate	10 MHz
BW of LPF	5 MHz
Number of runs	4000
N	2
K	0
Θ_{lim}	2°

On Figure 4-14 AOA RMS error is given as function of SNR for the complex and envelope crosscorrelator. As seen on the figure the real crosscorrelator performs better than the complex crosscorrelator when the SNR is high. On the other hand when the SNR is low threshold effects occurs for envelope correlation due to the detectors used. Hence the complex correlation is better for low SNR cases. Since DF systems work on high SNR environments [1] envelope crosscorrelator is better for practical cases. As a result of the simulations given above envelope crosscorrelator is used in this thesis.

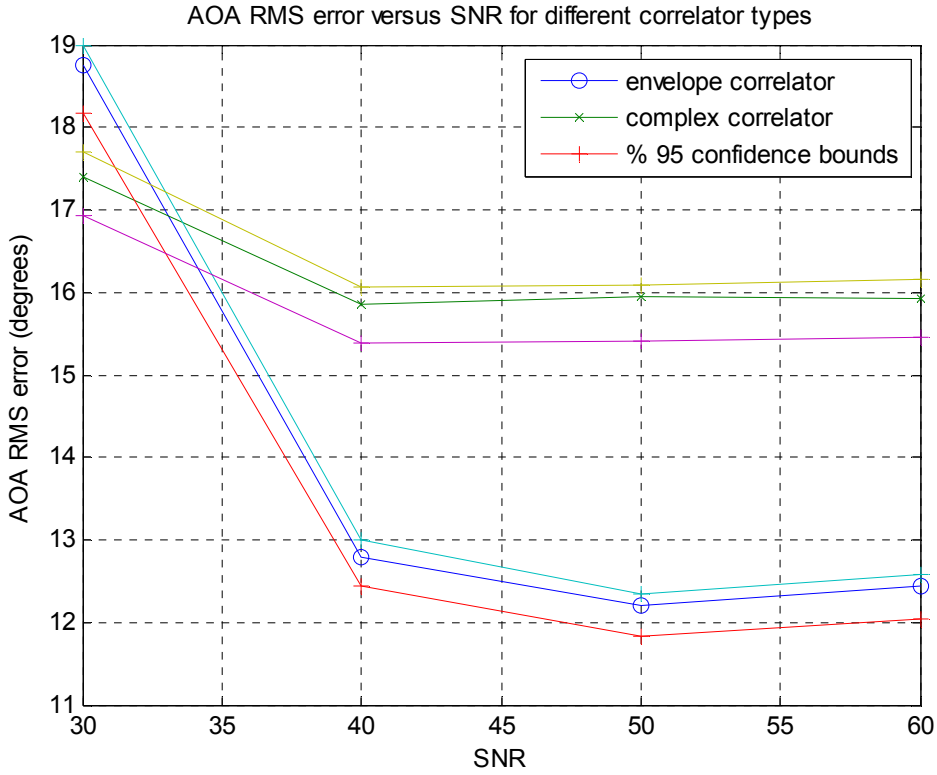

Figure 4-14: SNR versus AOA RMS Error for different crosscorrelator types at 2 μsec delayspread

4.3.2 Effect of Channel Parameters

Variation of the channel parameters also affects the AOA estimation performance. Channel parameters that affect the AOA estimation performance are:

1. Delayspread of the channel

2. Average power delay profile of the channel

4.3.2.1 Effect of Delayspread

Delayspread of a channel gives information about the amount of multipath in a channel. Thus change in delayspread of a channel also affects the AOA estimation performance. In order to observe the effects of delayspread on estimation performance, Monte Carlo simulations with parameters given in Table 4-5 are carried out.

Table 4-5: Simulation parameters for observing effect of delayspread

Source signal	A rectangular radar pulse of pulsewidth 4.5μsec
Average power delay profile	Exponential power delay profile $e^{-t/\tau_c}u(t)$
Delay spread for channel 1	Changed from 1 μsec to 7 μsec
Delay spread for channel 2	Changed from 1 μsec to 7 μsec
Observation time	15 μsec
Doppler spread	Ignored
Signal AOA	60°
SNR	Changed from 10 dB to 60 dB
Distance between sensor sites	750 m
Sampling rate	10 MHz
BW of LPF	5 MHz
Number of runs	4000
n	2
K	0
Θ_{lim}	2°

On Figure 4-15, Figure 4-16 and Figure 4-17, standard deviation, gross error probability and bias are given as functions of delayspread of channel 1 and channel 2. The reason for using the standard deviation as a performance criterion

is the increasing of bias (Figure 4-17) with an increase in difference of delayspread between channels. This effect can be seen on Figure 4-17. As seen on Figure 4-15 standard deviation increases with increasing delayspread. Moreover as seen on Figure 4-16 when then delayspread of one channel is kept constant and delayspread of the other is decreased, gross error probability does not decrease due to the bias effect at unequal delayspread of the channels.

On Figure 4-18 AOA RMS error is given as function SNR for delayspread of channel 1 and channel 2 are equal to 2 μsec. As seen on the figure after 40 dB SNR, AOA RMS error does not decrease for increasing SNR. This shows that there is threshold effect due to multipath channel. The threshold effect occurs due to fluctuation in the channel. Moreover the reason for gross error probability is also fluctuations in the channel. In order to show the affect of channel fluctuation on crosscorrelation function, crosscorrelation functions for singlepath and multipath channels is given in Figure 4-19. As a result performance of the system is limited by fluctuation in the channel in addition to thermal noise.

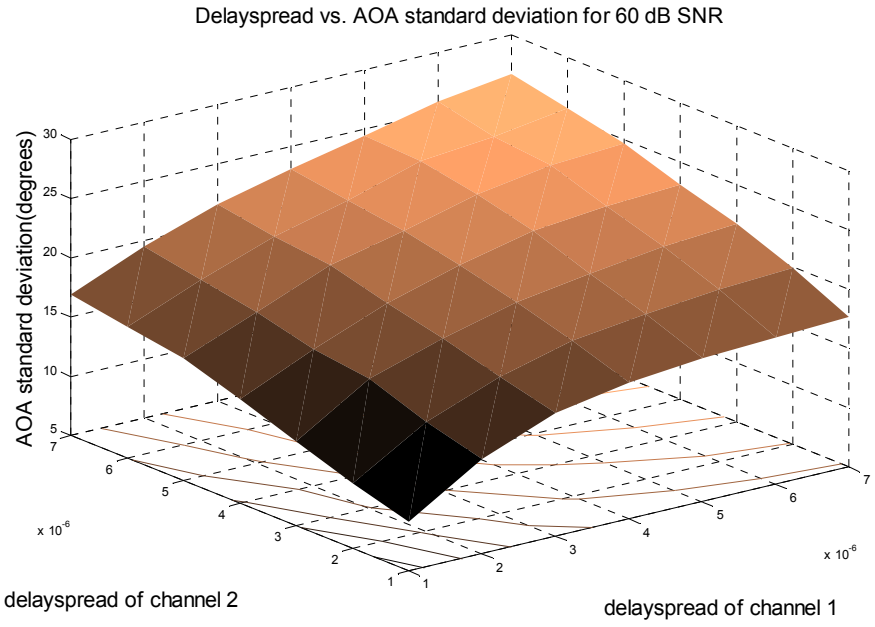

Figure 4-15: Delayspread versus standard deviation at 60 dB SNR

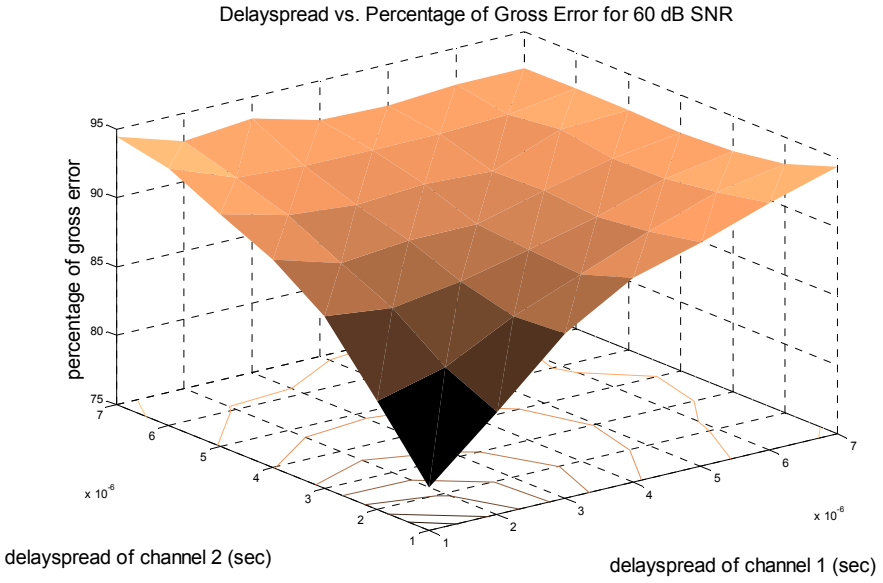

Figure 4-16 : Delayspread versus percentage of gross error at 60 dB SNR

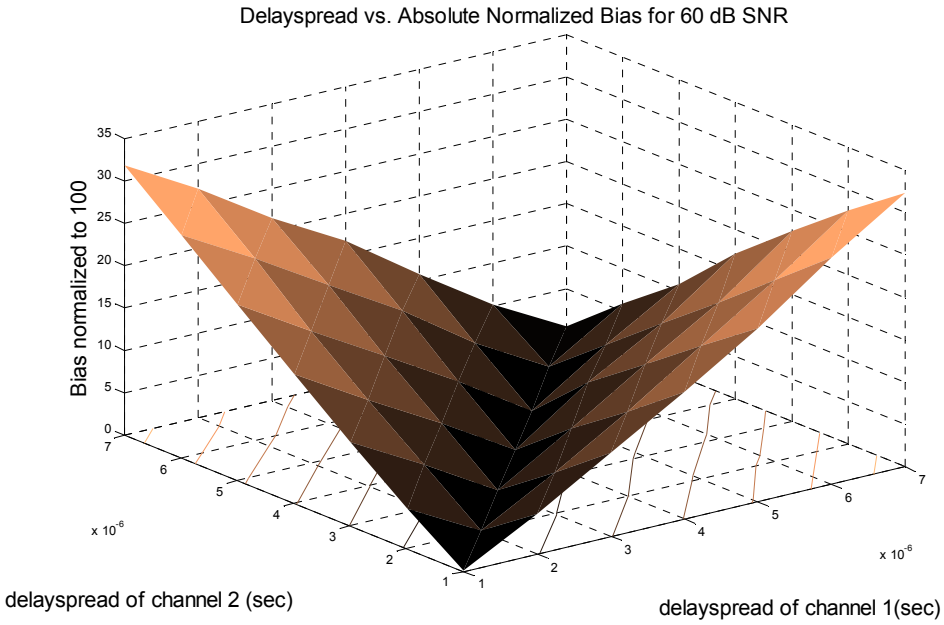

Figure 4-17: Delayspread versus absolute normalized bias at 60 dB SNR

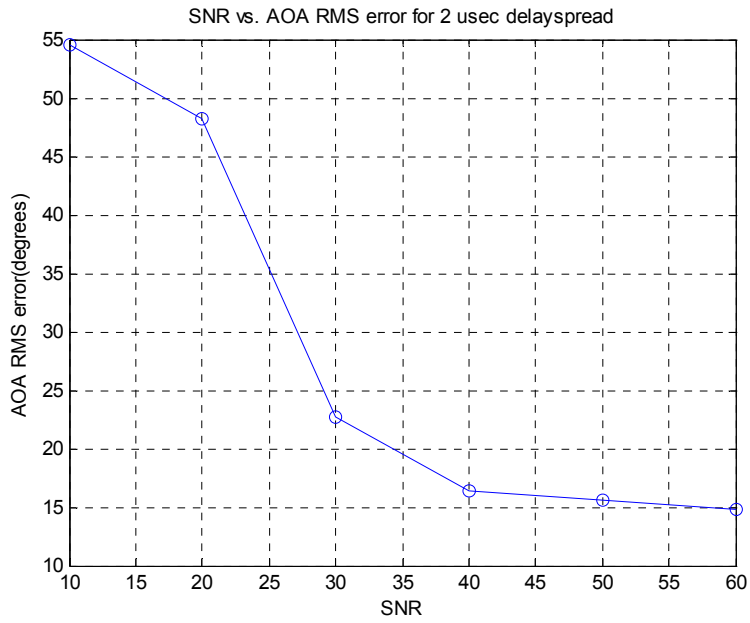

Figure 4-18: SNR versus AOA RMS error for 2µsec delayspread

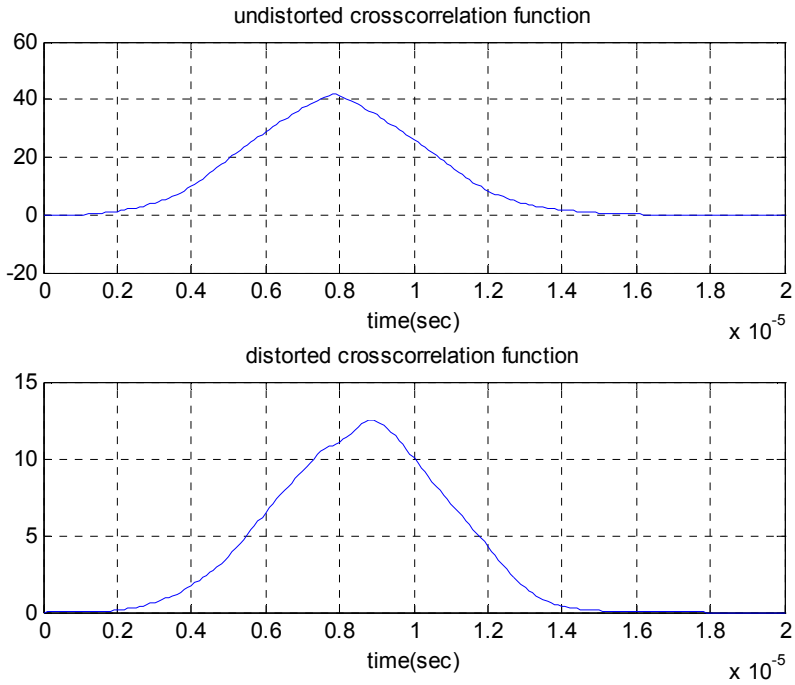

Figure 4-19: Undistorted and distorted cross correlation functions

4.3.2.2 Average Power Delay Profile of the Channel

Average power delay profile of the channel also affects the AOA estimation performance. Effect of average channel delay profile is analyzed for following cases:

- Effect of Power of LOS signal component for exponential power delay profile
- Effect of hilly terrain power delay profile compared to exponential power delay profile.

4.3.2.2.1 Effect of Power of LOS Signal Component for Exponential Power Delay Profile

Presence of LOS component in the received signal affects the AOA estimation performance. When there is a LOS path in the environment then the channel is Ricean, else it is Rayleigh, [27]. In order to show the effect of power of LOS component in the received signal Monte Carlo simulation with parameters given in Table 4-6 is carried out.

Table 4-6: Simulation parameters for observing effect of LOS signal on estimation performance

Source signal	A rectangular radar pulse of pulse width 4.5μsec
Average power delay profile	Exponential power delay profile $e^{-t/\tau_c}u(t)$
Delay spread	2 μsec
Observation time	15 μsec
Doppler spread	Ignored
Signal AOA	60°
SNR	Changed from 10 dB to 60 dB
Distance between sensor sites	750 m
Sampling rate	10 MHz
BW of LPF	5 MHz
Number of runs	4000
n	2
K	Changed from 0 to 25
Θ_{lim}	2°

On Figure 4-20 and Figure 4-21 AOA RMS error and gross error probability are given as a function of K. As shown on the figures, as the ratio of the power of LOS signal to the total power of scattered signals increases, AOA RMS error and probability of gross error decrease. Here it is notable that as power of LOS signal increases, gross error in the RMS error decreases remarkably.

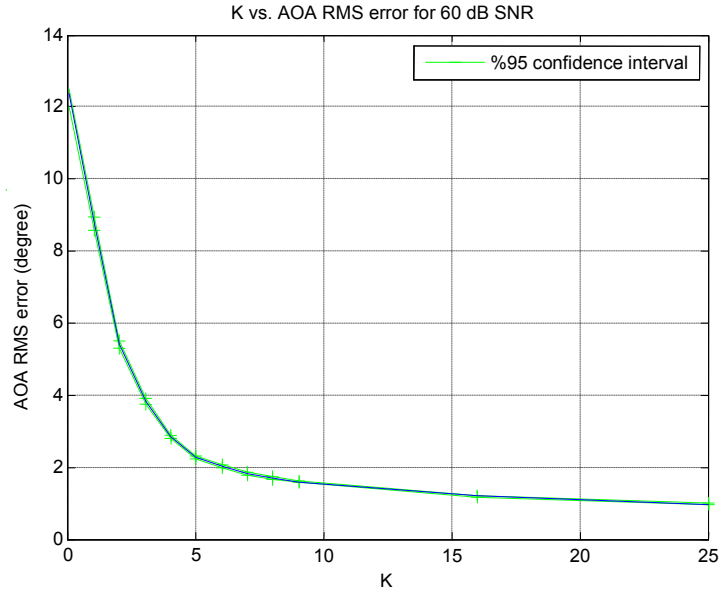

Figure 4-20: *K* versus AOA RMS error for 60 dB SNR

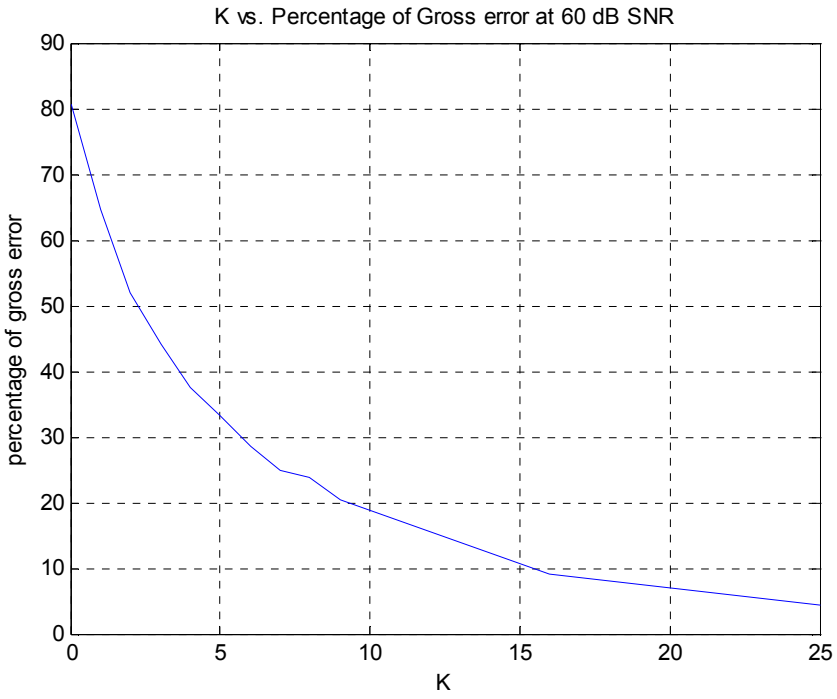

Figure 4-21: *K* versus Percentage of Gross error for 60 dB SNR

4.3.2.2.2 Effect of Hilly Terrain Power Delay Profile Compared to Exponential Power Delay Profile.

Shape of the average power delay profile affects the AOA estimation performance. When the propagation environment is hilly terrain, shape of the average power delay profile is modeled by 2 exponential functions on the other hand when the propagation environment is rural; shape of the average power delay profile is modeled by only one exponential. In order to show the effect shape of power delay profile Monte Carlo simulation with parameters given in Table 4-7 is carried out.

Table 4-7: Simulation parameters for observing the effect of the average power delay profile shape

Channel type	Rural	Hilly terrain
Source signal	A rectangular radar pulse of pulse width 4.5 μsec	A rectangular radar pulse of pulse width 4.5 μsec
Average power delay profile	$e^{-t/\tau_c}u(t)$	$e^{-t/\tau_c}u(t)+0.8$ $e^{-(t-1.5\mu\sec)/\tau_c}u(t-1.5\mu\sec)$
Delay spread	2 μsec	2 μsec
Observation time	15 μsec	15 μsec
Doppler spread	Ignored	Ignored
Signal AOA	60°	60°
Distance between sensor sites	750 m	750 m
Sampling rate	10 MHz	10 MHz
BW of LPF	5 MHz	5 MHz
Number of runs	4000	4000
n	2	2
K	0	0
Θ_{lim}	2°	2°

On Figure 4-22 and Figure 4-23 AOA RMS error and gross error are given as function of energy SNR for rural and hilly terrain average power delay profiles respectively. As shown on the figure performance in rural area outperforms the performance in hilly terrain area. This is reasonable since the faraway reflector in hilly terrain rural environment creates an ambiguous peak in correlation function and this increase the gross error.

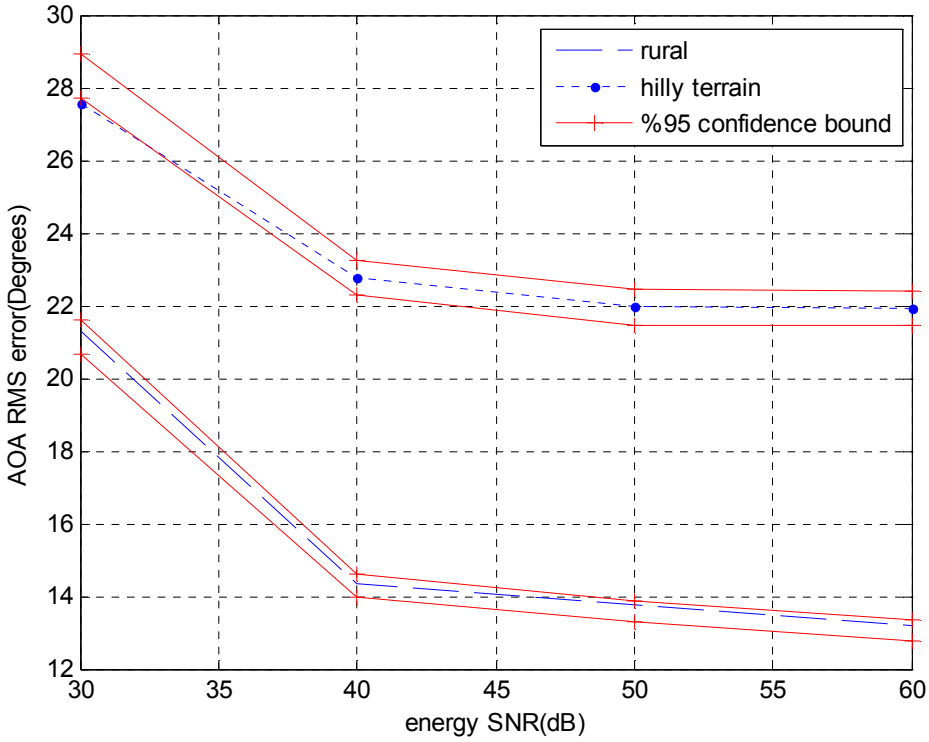

Figure 4-22: SNR versus AOA RMS error for 2 μsec delayspread

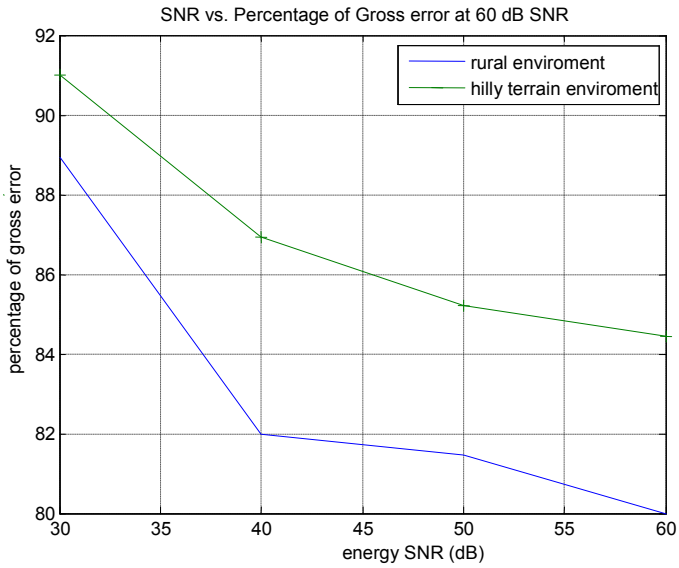

Figure 4-23: SNR versus Percentage of Gross error for 2 μsec delayspread

4.3.3 Effect of Radar Parameters

Radar parameters also affect the AOA estimation performance. Parameters which affect the performance are:

- AOA of the radar signal
- Pulsewidth of the radar signal.

4.3.3.1 AOA of the Radar Signal

AOA of the signal affects performance of the estimation. This is because the derivative of $sin^{-1}()$ in equation (3-16) is strictly increasing with increasing argument. In order to show this effect Monte Carlo simulations with parameters given in Table 4-8 are carried out. It is important to note that AOA estimation performance curves are symmetric for AOA range of [-90°, 90°] since absolute values of the TDOAs are same for positive and negative AOAs. Hence on the simulations AOA range of [0°, 90°] is used.

Table 4-8: Simulation parameters for observing the effect of the AOA of radar signal

Source signal	A rectangular radar pulse of pulse width 4.5μsec
Average power delay profile	Exponential power delay profile $e^{-t/\tau_c}u(t)$
Delay spread	2 μsec
Observation time	15 μsec
Doppler spread	Ignored
Signal AOA	Changed from 0° to 85°
SNR	Changed from 10 dB to 60 dB
Distance between sensor sites	750 m
Sampling rate	10 MHz
BW of LPF	5 MHz
Number of runs	4000
n	2
K	0
Θ_{lim}	2°

On Figure 4-24 and Figure 4-25 AOA RMS error and percentage of gross error are given as a function of AOA respectively. As shown on the figures AOA RMS error and percentage of gross error are increasing with increasing AOA. After 30° it is observed that the slope of the curve in on Figure 4-24 increase due to increasing derivative of $sin^{-1}()$. In order to solve this problem one possible approach may be using synchronously rotating antennas with 3 dB beamwidths smaller than 60° in the system.

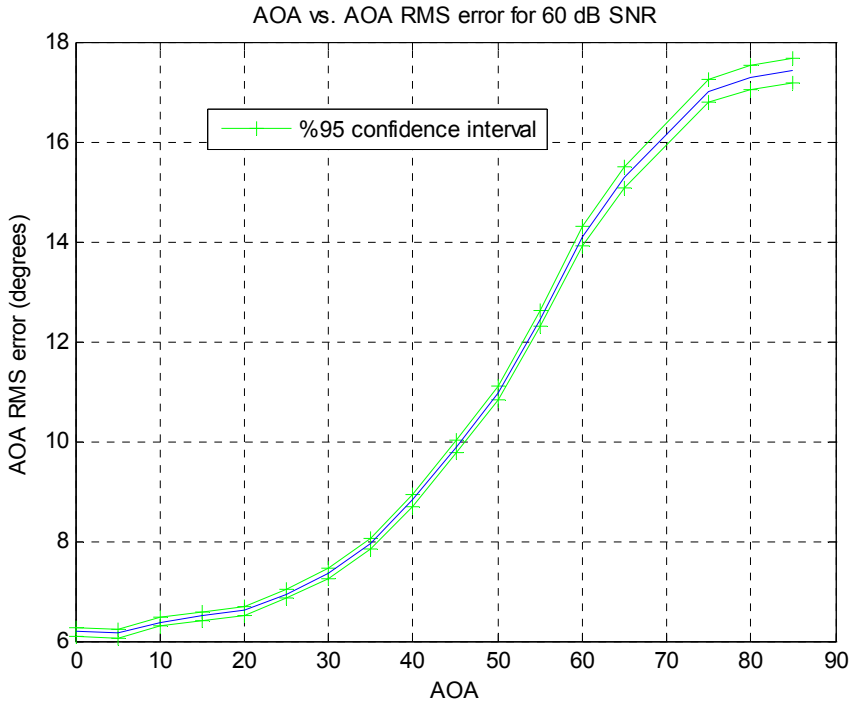

Figure 4-24: AOA versus AOA RMS error at 60 dB SNR

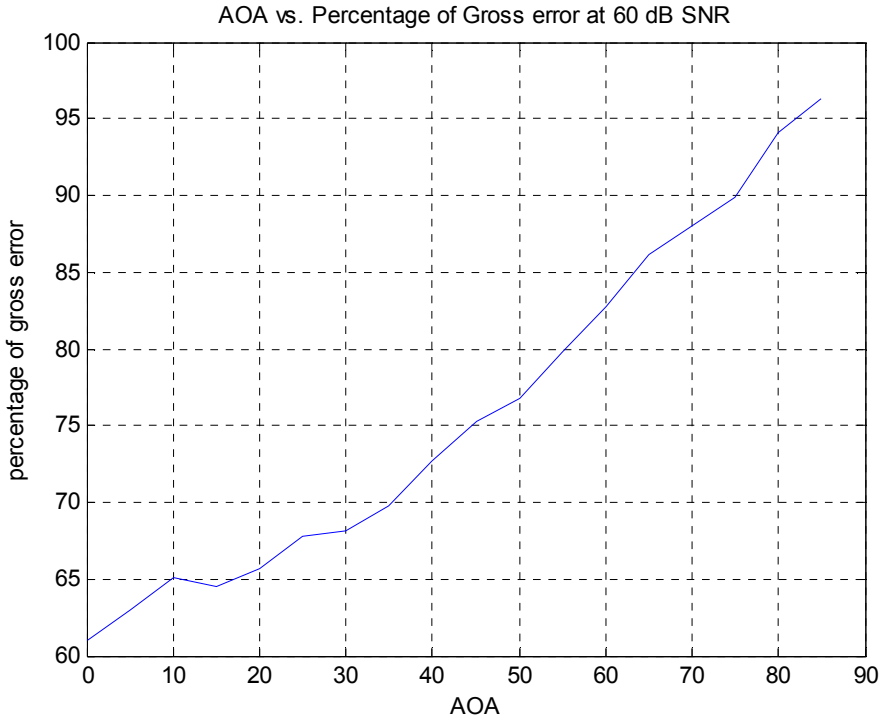

Figure 4-25: AOA versus Percentage of Gross error at 60 dB SNR

4.3.3.2 Pulsewidth of the Radar Signal

Pulsewidth affects the range resolution of radar. Range resolution is proportional with pulsewidth. Pulsewidth of the radar also affects the performance of AOA estimation of the DF system proposed in this thesis. In order to observe the effects of pulsewidth Monte Carlo simulations with parameters given Table 4-9 are carried out.

Table 4-9: Simulation parameters for observing the effect of the pulsewidth of radar signal

Source signal pulsewidth	Changed from 0.5 μsec to 9 μsec
Average power delay profile	Exponential power delay profile $e^{-t/\tau_c}u(t)$
Delay spread	Changed from 2 μsec to 9 μsec
Observation time	15 μsec
Doppler spread	Ignored
Signal AOA	60°
SNR	Changed from 10 dB to 60 dB
Distance between sensor sites	750 m
Sampling rate	10 MHz
BW of LPF	5 MHz
Number of runs	4000
n	2
K	0
Θ_{lim}	2°

On Figure 4-26 and Figure 4-27 AOA RMS error and percentage of gross error are given as a function of pulsewidth for 60 dB SNR. As seen on the figures when pulsewidth is increased, AOA RMS error and percentage of gross error increase until pulsewidth value comes close to delayspread value. When pulsewidth is

greater than delayspread value AOA RMS error and percentage of gross error is in steady state. When pulsewidth is smaller than delayspread, increase on the pulsewith distorts the signal.

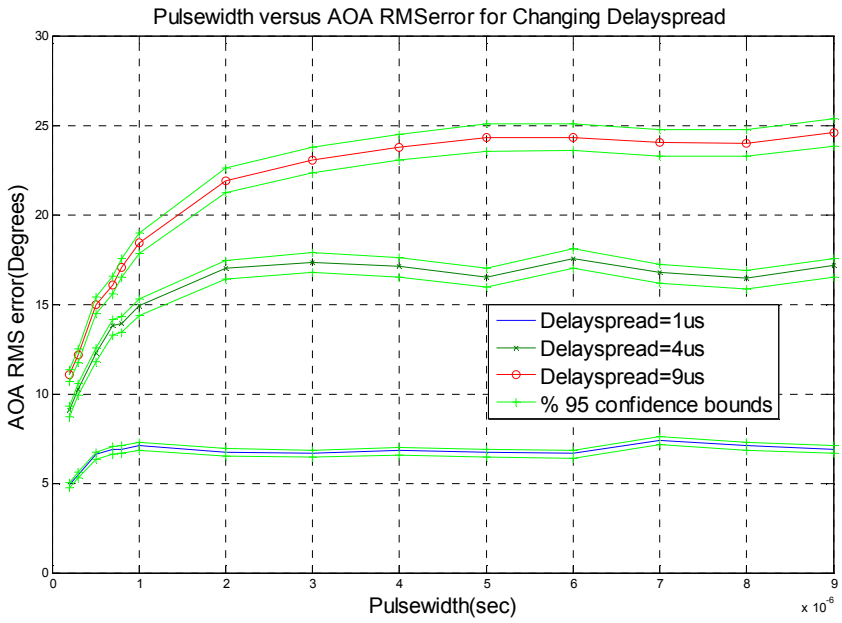

Figure 4-26: Pulsewidth versus AOA RMS error for changing delayspread

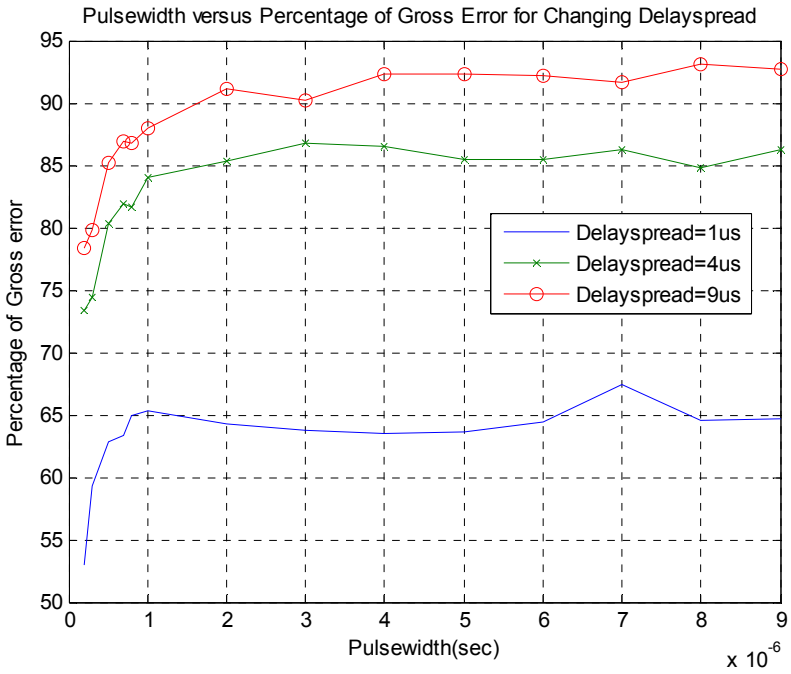

Figure 4-27: Pulsewidth versus Percentage of Gross Error for changing delayspread

CHAPTER 5

IMPACT OF DIVERSITY

As observed in the previous chapter multipath channel degrades the AOA estimation performance. Effects of multipath channel can be partially eliminated by the utilization of diversity on the receivers. In order to investigate the improving effects of diversity on AOA estimation performance first diversity techniques in the literature and their applicability to the problem given in thesis is discussed, then the modification to the system model and simulation methodology is discussed. Finally, results of Monte Carlo simulations are presented.

5.1 Diversity Methods

The diversity methods in the literature are mainly derived for communication systems. Hence only a portion of the diversity techniques are applicable. In order to determine which techniques are applicable to the problem of this thesis, first diversity techniques that are applied on receivers are investigated then the applicability of these techniques to the problem given in this thesis is discussed.

5.1.1 Diversity Techniques in Literature

Diversity techniques used in the literature are given below, [28], [29]:

1. Rake Receiver

Rake receiver aims to align the delayed replicas of the transmitted signal in time domain and sum the aligned signal in order to have a diversity gain. System model for rake receiver is given in Figure 5-1.

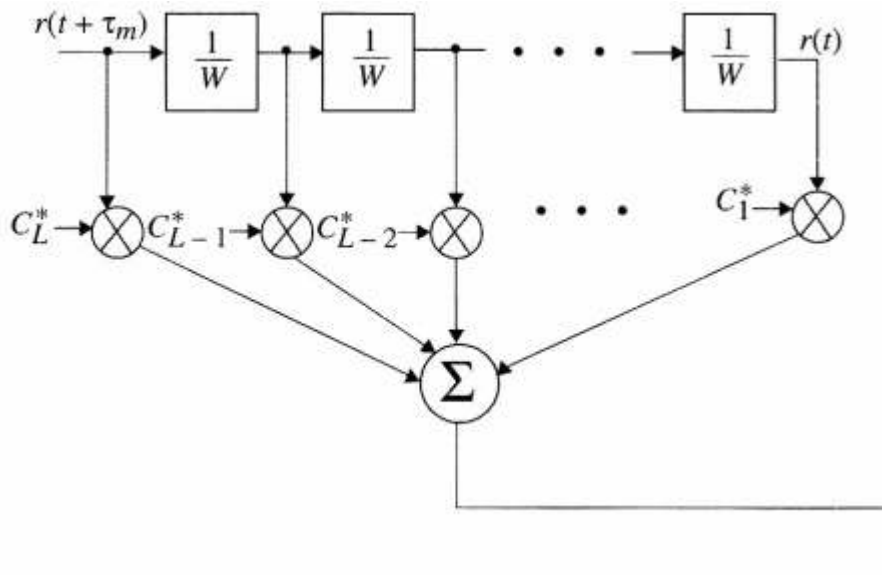

Figure 5-1: System model using rake receiver, [29]

2. Space diversity with selective combining (SC)

Model of the system using space diversity with SC is given in Figure 5-2

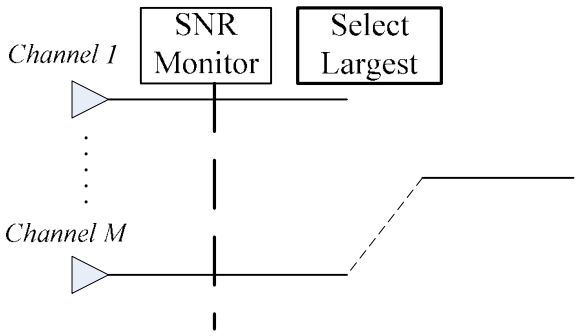

Figure 5-2: System model using space diversity with SC

If SNR of the received signal can be estimated, space diversity with SC is applied by choosing the branch with the highest SNR. When SNR information

is not available, channel with the highest power can be used for branch selection criterion.

3. Space diversity with equal gain combining (EGC)

Model of the system which uses the space diversity with EGC is given in Figure 5-3.

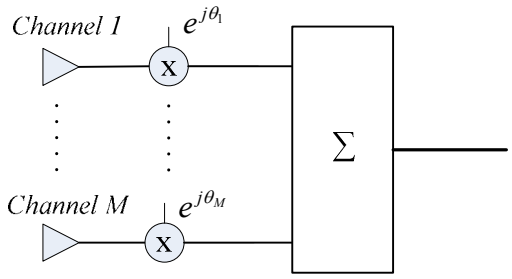

Figure 5-3: System model using space diversity with EGC

In this method signals from M branches are co-phased and summed.

4. Space diversity with maximal ratio combining (MRC)

Model of the system which uses the space diversity with MRC is given in Figure 5-4.

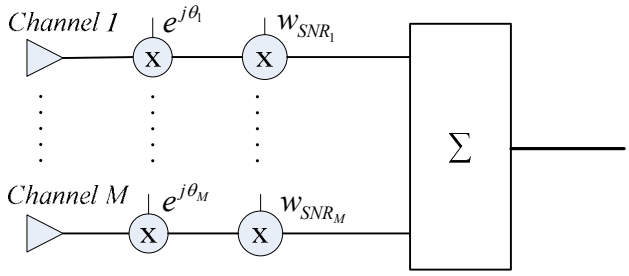

Figure 5-4: System model using space diversity with MRC

In this method signals from M branches are first co-phased then weighed according to their individual SNRs and added.

5. Space diversity with noncoherent combining(NC)

Model of the system using space diversity with NC is given in Figure 5-5.

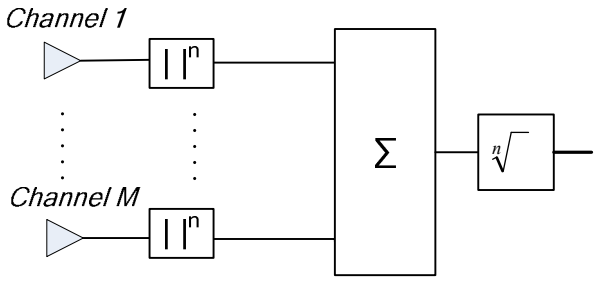

Figure 5-5: System model using space diversity with NC

In this method signals from M branches first detected with n^{th} order envelope detector, then summed.

5.1.2 Applicability of the Diversity Methods:

The critical assumptions in order to determine the applicable diversity technique is written below:

1. Emitted radar signal is assumed to be nonrandom.
2. Phase of the received signal is not known
3. Channel is unknown

Due to the assumptions given above, diversity techniques that are not applicable to the problem given in this thesis are given in Table 5-1.

Table 5-1: Applicability of diversity combining methods

Diversity method	Violated Assumption		
	1	2	3
Rake Receiver	‡	‡	
Space diversity with maximal ratio combining (MRC)	‡	‡	‡
Space diversity with equal gain combining (ECG)	‡	‡	
Space diversity with noncoherent combining (NC)			
Space Diversity with selective combining (SC)			

Since Space Diversity with NC and Space Diversity with SC do not violate any of the assumptions, they are applicable to the problem given in this thesis.

5.2 Modifications to the System Model

Since diversity is used in the system, receiver structure is modified as given in Figure 5-6.

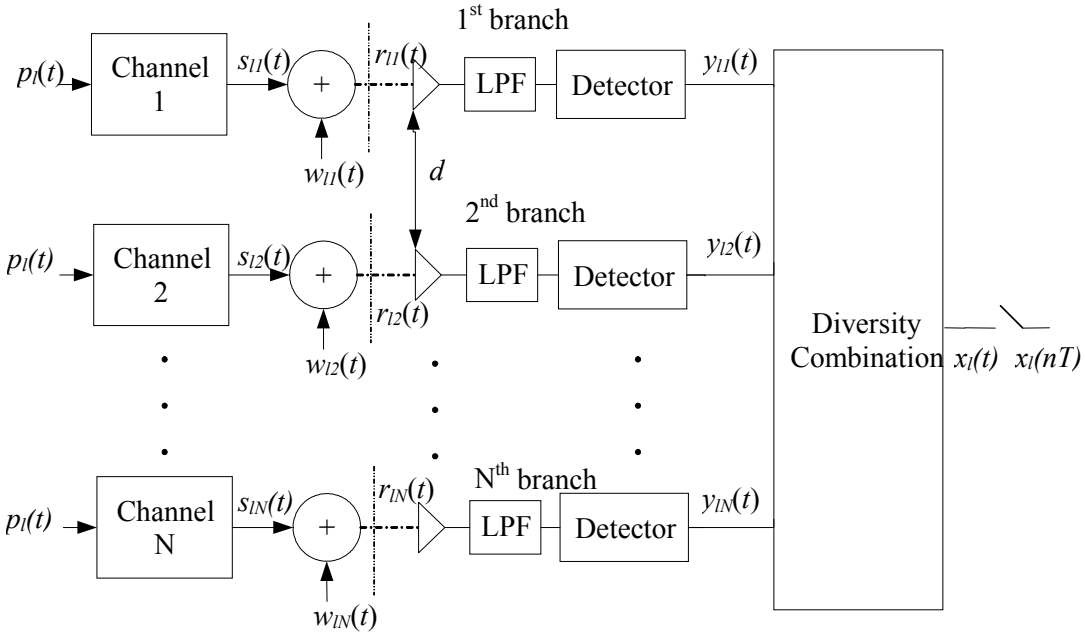

Figure 5-6: Modified system model

Critical assumptions used in the modified system model are given below:

- $d \geq 10\lambda$ (λ: wavelength of the received signal) for independence of the channels

- $N < \frac{\Theta * c}{10d} + 1$ (Θ: TDOA estimation resolution of the system) for the assumption of TDOA between array elements in a sensor site is equal to zero. Derivation of this expression is given in Appendix D.

In the expressions given above, *d* is the distance between sensor in an array and *N* is the number of sensors in a sensor array. Moreover the second assumption is used to determine the maximum number of diversity antennas.

5.3 Modification to the Simulation Methodology

In order to apply the SC and NC diversity methods in Monte Carlo simulations, simulation methodology has to be modified. Modification in simulation methodology is done on the signal generation part. For SC and NC modified signal generation methods are given below:

5.3.1 Signal Generation when Space Diversity with NC is used

1. Radar pulse, $p(t)$ is generated
2. Number of diversity branches, N is set
3. N channels are generated.
4. Generated radar pulse is passed through the channels and additive white Gaussian noise is added to each. As a result noisy signals $y_1(t), y_2(t)....y_N(t)$ are generated
5. $y_1(t), y_2(t)....y_N(t)$ are combined according to the formula: $x_l(t) = \sqrt[n]{|y_1(t)|^n + |y_2(t)|^n + ... + |y_N(t)|^n}$

5.3.2 Signal Generation when Space Diversity with SC is used

1. Radar pulse, $p(t)$ is generated
2. Number of diversity branches, N is set
3. N channels are generated.
4. Generated radar pulse is passed through the channels and additive white Gaussian noise is added. As a result noisy signals $y_1(t), y_2(t)....y_N(t)$ are generated

5. The maximum power level of each branch during the observation interval is found,
6. Power levels found in step 5, are compared
7. The branch which has the highest power is selected.

5.3.3 Simulation Results

In order to investigate the improving effects of diversity on the AOA estimation performance Monte Carlo simulations are carried out. In Monte Carlo simulations following aspects of diversity are investigated:

- Effect of diversity combining technique on the estimation performance
- Effect of number of antennas
- Effect of detector order on the AOA performance when space diversity with NC is used

Furthermore, the parameters given in section 4.3 also affect the estimation performance, when diversity is applied. Since diversity gives an improvement in estimation performance, the effect of parameters given in section 4.3 on the estimation performance does not change.

5.3.4 Effect of Diversity Combining Technique on the Estimation Performance

Diversity techniques that can be applied to the problem given in this thesis are defined in section 5.1.2. In order to observe the effect of application of diversity to the AOA estimation performance Monte Carlo simulations with parameters given in Table 5-2 are carried out.

Table 5-2: Simulation parameters for observing effect of diversity combination technique on estimation performance

Diversity technique	NC Diversity	SC Diversity	No diversity
Source signal	A rectangular radar pulse with pw 4.5 µsec	A rectangular radar pulse with pw 4.5 µsec	A rectangular radar pulse with pw 4.5 µsec
Number of branches (N)	10	10	1
Average power delay profile	$e^{-t/\tau_c}u(t)$	$e^{-t/\tau_c}u(t)$	$e^{-t/\tau_c}u(t)$
Delayspread	Changed from 0 µsec to 5 µsec	Changed from 0 µsec to 5 µsec	Changed from 0 µsec to 5 µsec
Observation time	15 µsec	15 µsec	15 µsec
Doppler spread	Ignored	Ignored	Ignored
Signal AOA	60°	60°	60°
Baseline	750 m	750 m	750 m
Sampling rate	10 MHz	10 MHz	10 MHz
BW of LPF	5 MHz	5 MHz	5 MHz
Number of runs	4000	4000	4000
SNR	60 dB	60 dB	60 dB
n	2	2	2
K	0	0	0
Θ_{lim}	2°	2°	2°

On Figure 5-7 and Figure 5-8 AOA RMS error and percentage of gross error are given as function of delayspread for two different diversity combining techniques. As seen on the figure space diversity with NC outperforms space diversity with SC and no diversity cases. This is reasonable since space diversity with NC combine all of the branches whereas space diversity with SC uses only the branch with the highest power.

Obvious cause of performance improvement with space diversity with NC is SNR gain. In [30] it is shown that noncoherent integration with N pulses has an SNR gain upto $N^{0.8}$. Another cause of the performance improvement with space diversity with NC is smoothing of the impulse response of the channel. As discussed earlier, fluctuations on the response of multipath channel cause gross errors. When the sensor outputs are combined noncoherently, variance of the channel taps decrease, and this decreases fluctuation in the channel response. This is shown in Appendix E.

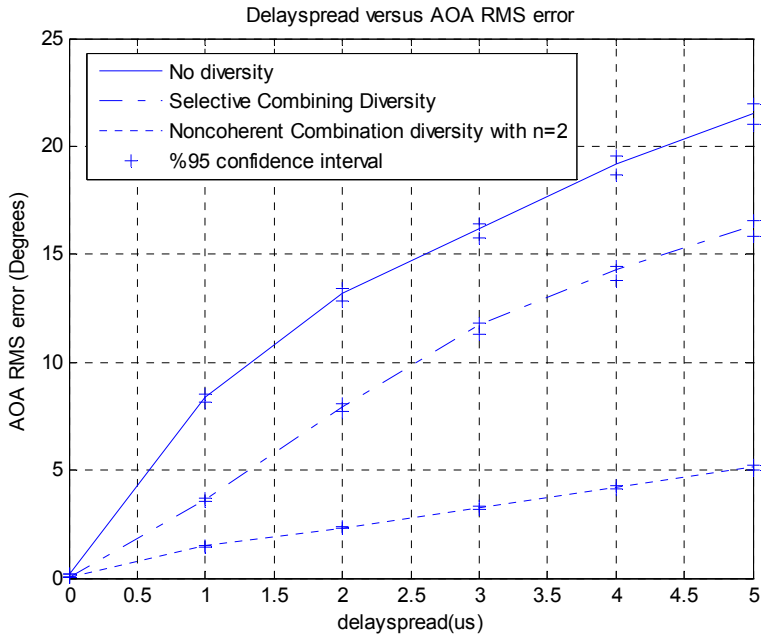

Figure 5-7 : Delayspread versus AOA RMS error for 60 dB SNR

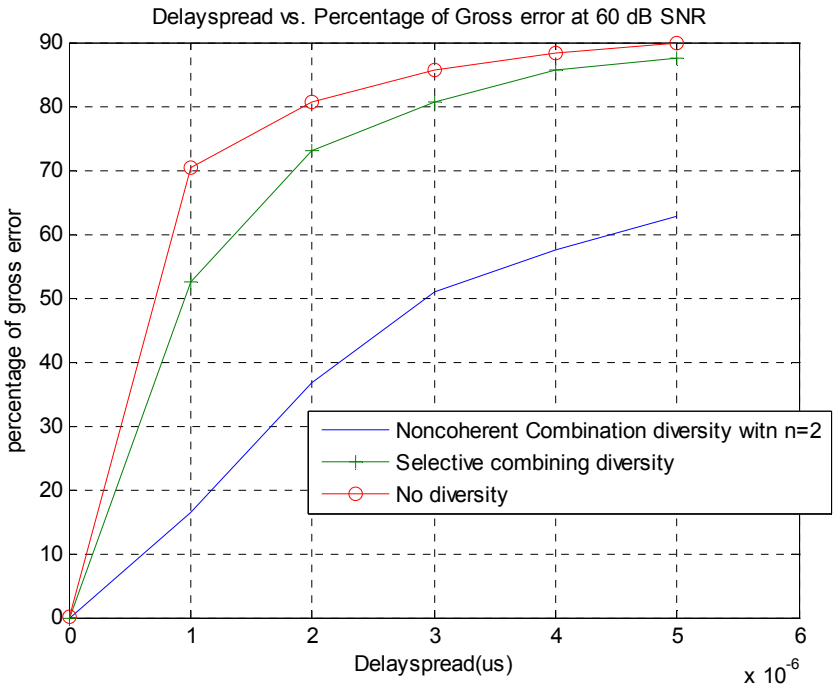

Figure 5-8: Delayspread versus Percentage of Gross error for 60 dB SNR

5.3.4.1 Effect of Number of Diversity Branches

Number of diversity branches affects the AOA estimation performance. In order to see the effect number of antennas on AOA estimation performance Monte Carlo simulations with parameters given in Table 5-3 are carried out.

Table 5-3: Simulation parameters for observing effect of number of diversity branches on estimation performance

Diversity technique	Noncoherent Combination Diversity	Selective Combining Diversity
Source signal	A rectangular radar pulse with pulsewidth 4.5 μsec	A rectangular radar pulse with pulsewidth 4.5 μsec
Number of branches(N)	Changed from 1 to 10	Changed from 1 to 10
Average power delay profile for all channels	$e^{-t/\tau_c}u(t)$	$e^{-t/\tau_c}u(t)$
Delay spread	2 μsec	2 μsec
Observation time	15 μsec	15 μsec
Doppler spread	Ignored	Ignored
Signal AOA	60°	60°
Distance between sensor sites	750 m	750 m
Sampling rate	10 MHz	10 MHz
BW of LPF	5 MHz	5 MHz
Number of runs	4000	4000
SNR	60 dB	60 dB
n	2	2
K	0	0
Θ_{lim}	2°	2°

On Figure 5-9 AOA RMS error is given as a function of number of diversity branches for Space Diversity with NC and SC. For space diversity with NC and SC slopes of the curves decrease after N=4 and N=6 respectively. This shows that after a certain N value, gain in performance decreases. Then if the cost of diversity branches is important, the best values for N are 4 and 6 for Space Diversity with NC and SC respectively.

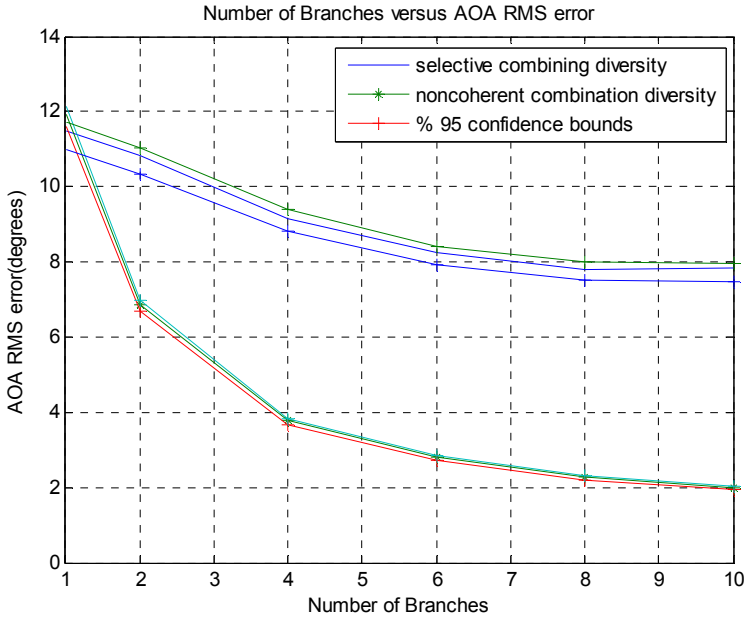

Figure 5-9: Number of diversity branches versus AOA RMS error for 60 dB SNR and 2 μsec delayspread

5.3.4.2 Effect of Detector Order

As discussed in section 3.3.4, order of the detector is a design parameter. In order to see the effect of detector order on AOA estimation performance, Monte Carlo simulations with parameters given in Table 5-4 are carried out.

Table 5-4: Simulation parameters for observing effect of detector order on estimation performance

Diversity technique	Noncoherent Combination Diversity
Source signal	A rectangular radar pulse with pulse width 4.5 μsec
Number of branches(N)	10
Average power delay profile for all channels	$e^{-t/\tau_c}u(t)$
Delay spread	2 μsec
Observation time	15 μsec
Doppler spread	Ignored
Signal AOA	60°
Distance between sensor sites	750 m
Sampling rate	10 MHz
BW of LPF	5 MHz
Number of runs	4000
SNR	60 dB
n	1,2,3,4

On Figure 5-10 AOA RMS error is given as a function of detector order. As seen on the figure best performance is obtained when the detector order is 2. This is expectable since the performance criterion is RMS error.

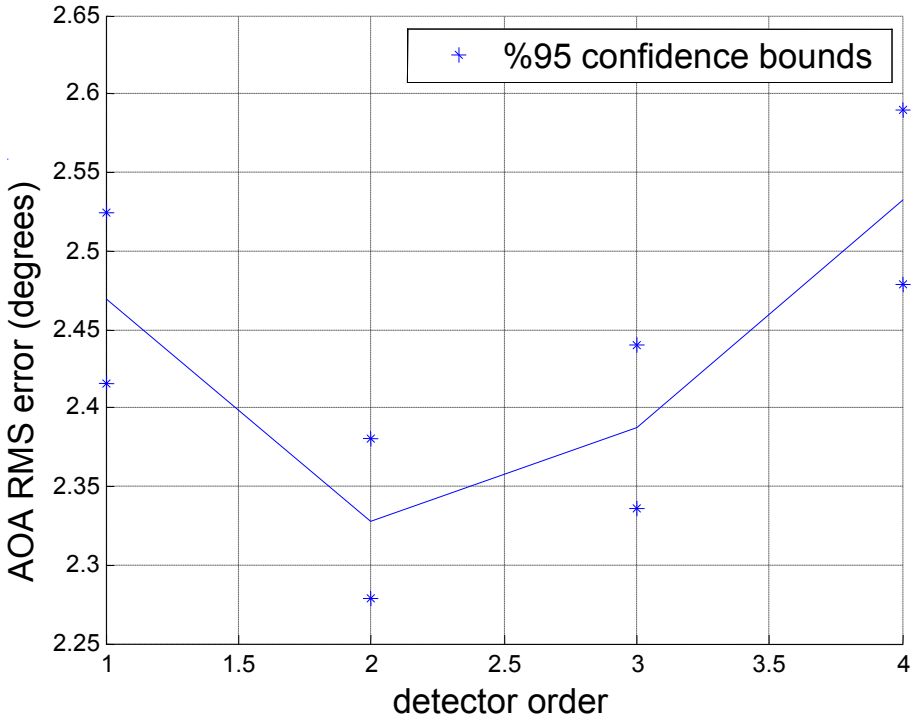

Figure 5-10: Detector order versus AOA RMS error for 60 dB SNR and 2 μsec delayspread

CHAPTER 6

A REALISTIC SCENARIO

In chapters 4 and 5, performance of the proposed system is investigated by variation of system, radar and channel parameters one by one. The aim of the Monte Carlo simulations in chapter 4 and 5 were determining the desired system, radar and channel parameters. In this section a realistic scenario will be designed with results of chapter 4 and 5. Moreover the performance of the proposed system will be observed in the designed scenario.

6.1 Scenario

Let the radar and the DF system is located as shown in Figure 6-1.

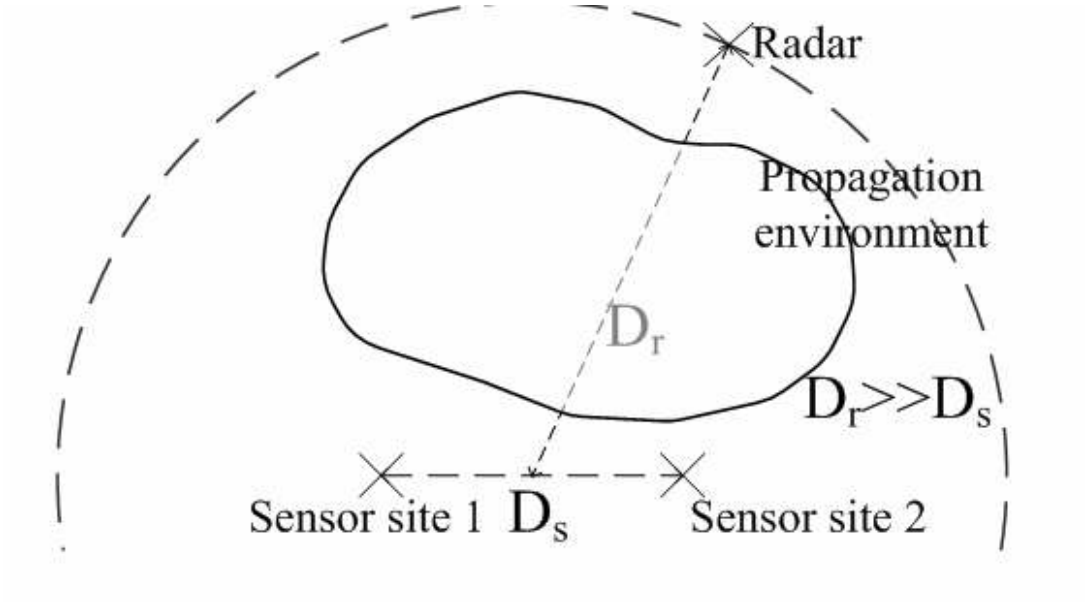

Figure 6-1: Location of the radar and the DF system

D_r and D_s on Figure 6-1 are distance between radar and sensor sites, and distance between sensor sites respectively. In order to apply TDOA method, D_r has to be much greater then D_s. Propagation environment between the radar and sensor sites is hilly terrain. The environment between radar and sensor sites can be modeled as given in Figure 6-2

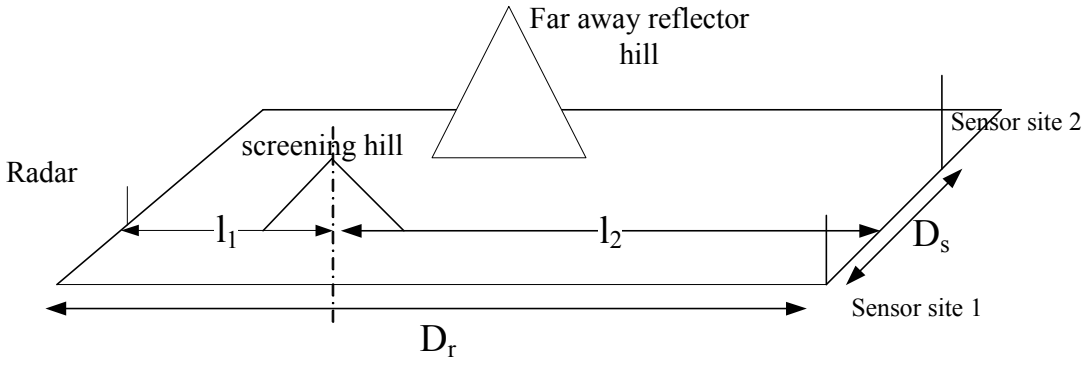

Figure 6-2: Model of the environment

As shown in Figure 6-2 radar is located behind a screening hill in order to decrease the probability of detection. Radar is a land based radar with output power 100 W,

pulsewidth 1μsec, transmitting antenna gain 30dB and transmitting frequency 10 GHz. Its height is taken to be 10 m form the ground, whereas the height of the screening hill is 30 m. Radar's distance to screening hill is taken to be 1000m. Also there is a far away reflector hill in the environment. Hence the environment is hilly terrain environment. Moreover the receivers are located 19 km from the screening hill and their sensitivity is taken to be -75 dBm. Since the rest of the receiver parameters are design parameters, their selection will be discussed in next section.

If it is assumed that the channel does not put any gain to the transmitted signal, the energy of the received signal can be written as

$$E_r = P_r * pw = \frac{G_t G_r \lambda^2}{(4\pi D_r)^2} * P_t * |F|^2 * pw \qquad (6\text{-}1)$$

where F is the attenuation introduced by the propagation environment in addition to the free space path loss. If the environment is NLOS, F can be derived by Knife-Edge Diffraction model.

- Knife-Edge Diffraction Model, [31]

A knife-edge means a sharply defined obstacle opaque to, and placed in the way of, radio waves. With such an idealized diffracting edge, devoid of any electrical properties, the diffracted field at the receiver can be calculated by methods widely used in physical optics.

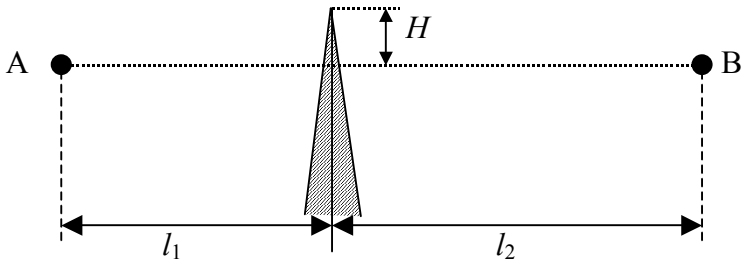

Figure 6-3: Propagation across a knife-edge.

Figure 6-3 shows the case of radio propagation across a knife-edge. The attenuation function is given by

$$F = \frac{1}{\sqrt{2}}\left[C(v) + jS(v)\right] \tag{6-2}$$

where $C(v)$ and $S(v)$ are Fresnel integrals defined as

$$C(v) = \frac{1}{2} - \int_0^v \cos\frac{\pi x^2}{2}\,dx; \quad S(v) = \frac{1}{2} - \int_0^v \sin\frac{\pi x^2}{2}\,dx \tag{6-3}$$

and the parameter v is given by

$$v = \frac{H\sqrt{2}}{b} \tag{6-4}$$

and b is the radius of the first Fresnel zone at the obstacle given by

$$b = \sqrt{\frac{l_1 l_2 \lambda}{l_1 + l_2}}. \tag{6-5}$$

6.2 Simulation Results

In order to observe the performance of the proposed system in a realistic scenario, Monte Carlo simulations will be carried out. First simulation parameter has to be determined. Most of the simulation parameters are determined according to consequences of the simulations carried out in chapters 4 and 5. Discussion on selection of radar, channel and system parameters are given below:

- Radar parameters: Since a DF system does not have control on radar parameters; they are given in scenario section. Only parameter that can be changed is AOA of the radar, because it's also related to the position of DF system. In section 4.3.3.1, it was shown that AOA smaller than 30° was desirable for the DF system, but in order to observe the AOA estimation performance at full angular coverage, the AOA is swept from 0° to 85°.

- Channel parameters: Channel is hilly terrain as described in scenario section. Average power delay profile function is given below:

$$e^{-t/\tau_c}u(t)+0.4e^{-(t-15\mu\sec)/\tau_c}u(t-15\mu\sec) \quad (6\text{-}8)$$

Delayspread of first and second exponentials are both 2 μsec and total delay spread is 17 μsec. Value of *K* parameter is 0. Finally Doppler spread is ignored.

- Receiver parameters: Sensor sites are at a height of 10 m from the ground. Distance between sensor sites is taken as 1000 m in order to satisfy the baseline criterion of the TDOA. There are 10 diversity antennas with 20 dB gains at each sensor site and space diversity with noncoherent combination is utilized. Detectors used in the receivers are square law as a result of section 5.3.4.1. Observation window length is taken as 20 μsec as a result of section 4.3.1.1. IF BW is taken as 5 MHz in order to improve time resolution. When thermal noise temperature is 300°, calculated energy SNR at the receiver with equation (6-1) is 68 dB.

On Figure 6-5 AOA RMS error is given as a function of AOA.

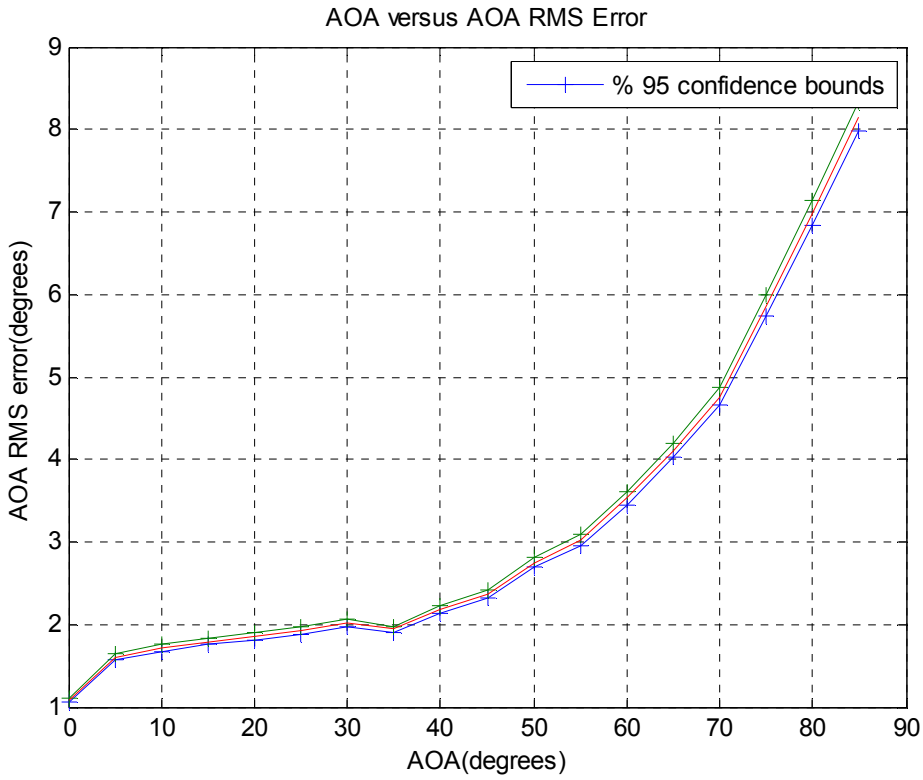

Figure 6-5: AOA versus AOA RMS error

2° AOA RMS error is a reasonable performance limit for an EW system in a land environment, [32]. On the figure it can be seen that below 40° AOA, AOA RMS error is below 2°. Thus it can be concluded that proposed DF system performs well in a multipath land environment upto an AOA of 40°.

CHAPTER 7

SUMMARY AND CONCLUSIONS

The aim of this thesis is to investigate the performance of AOA estimation with Monopulse TDOA in an outdoor land multipath environment with limited LOS. TDOA of two received radar signals is estimated at two separated sensor sites with cross correlation method. Then TDOA measurements are converted to AOA information.

At the beginning of this study AOA estimation methods in the literature are discussed and the reason for using Monopulse TDOA is explained. Then TDOA estimation method is investigated in depth and system model used in this thesis is presented.

After giving the background information about the thesis, the performance of the given system is evaluated through Monte Carlo simulations. Effect of channel parameters on estimation performance is observed. Furthermore effect of system and radar signal parameters on the estimation performance is investigated. As a result these simulations deteriorating effects of the multipath channel on estimation performance is observed. It was seen that the performance is limited by multipath environment even at high SNR cases, due to the fluctuation in the channel response. Moreover desired system and radar parameters are determined as a result of simulations.

In order to improve the performance of the proposed system, diversity is applied. Space Diversity with NC and Space Diversity with SC are found to be the applicable diversity combination methods to the proposed system. It was seen that Space Diversity with NC and Space Diversity with SC improves the estimation performance. Moreover Space Diversity with NC outperformed Space Diversity with SC. Space Diversity with NC smoothed the channel and this effect improved the performance considerably in addition to effect of SNR gain.

Lastly a realistic system scenario is implemented. AOA estimation performance of the proposed system is observed in realistic scenario.

As a future work following can be done:

- A lower bound which include the variances of the channel taps may be derived, and an expression which will show the amount of fluctuation on the channel can be extracted from this lower bound

- An interpolation technique which would work on TDOA estimation in multipath channel can be derived.

REFERENCES

[1] R. G. Wiley, “Electronic Intelligence: Interception of Radar Signals”, Norwood, MA: Artech House, 1985

[2] F. Arıkan, “Design of A Monopulse Amplitude Comparison DF Processor Using Maximum Likelihood Algorithm”, MSc. Thesis, Ankara, METU, 1992

[3] B. Champagne, S. Bédard and A. Stéphenne, "Performance of Time Delay Estimation in the Presence of Room Reverberation", IEEE Trans. on Speech and Audio Processing, vol.4, no.2, pp. 148-152, March. 1996.

[4] P. L. Feintuch, N. J. Bershad, F. A. Reed, "Time Delay Estimation Using the LMS Adaptive Filter-Dynamic Behaviour", IEEE Transactions on Acoustics Speech and Signal Processing, vol. 29, pp. 571-576, June 1981.

[5] H. C. So, "Spontaneous and Explicit Estimation of Time Delays in the Absence/Presence of Multipath Propagation," Ph.D. dissertation, Department of Electronic Engineering, The Chinese University of Hong Kong, 1995

[6] A. Dersan, “Passive Radar Localization by TDOA Measurements”, MSc. Thesis, Ankara, METU, 2001

[7] P. Stoica and R. Moses, “Introduction to Spectral Analysis”, Upper Saddle River, NJ: Prentice-Hall, 1997

[8] C. H. Knapp and G. C. Carter, “The Generalized Correlation Method for Estimation of Time Delay”, IEEE Transactions on Acoustics Speech and Signal Processing, vol. 24, pp. 320-327, August 1976.

[9] G. C. Carter, “Time Delay Estimation for Passive Sonar Processing”, IEEE Transactions on Acoustics Speech and Signal Processing, ASSP-29, p.p. 463–470, June 1981

[10] A. H. Quazi, “An Overview on the Time Delay Estimate in Active and Passive Systems for Target Localization”, IEEE Transactions on Acoustics Speech and Signal Processing, ASSP-29, p.p. 527–533, June 1981

[11] J. P. Ianniello, “Time Delay Estimation Via Crosscorrelation in the Presence of Large Estimation Errors”, IEEE Transactions on Acoustics Speech and Signal Processing, ASSP-30, p.p. 998–1003, December 1982

[12] B. Frielander, “On the Cramer-Rao Lower Bound for Time Delay and Doppler Estimation”, IEEE Transactions on Information Theory, vol. 30, pp. 575-580, May 1980

[13] G. Jacovitti and G. Scarano “Discrete Time Techniques for Time Delay Estimation”, IEEE Transactions on Signal Processing, vol. 41, pp. 525-533, February 1993

[14] R. E. Boucher and J. C. Hassab “Analysis of Discrete Implementation of Generalized Crosscorrelator”, IEEE Transactions on Acoustics Speech and Signal Processing, ASSP-29, p.p. 609–611, June 1981

[15] M. Jian, A. C. Kot and M. H. Er, "Performance Analysis of Time Delay Estimation in a Multipath Environment," in Proc. DSP 97, Santorini, Greece, 2-4 Jul 1997, pp. 919-922

[16] P. B. G. Ferguson and K. W. Lo, "Passive Ranging Errors Due to Multipath Distortion of Deterministic Transient Signals with Applications to the Localization of Small Arms Fire," J. of Acoust. Soc. Amer., vol.111, pp.117-128, January 2002.

[17] G. C. Carter, Ed., “Coherence and Time Delay Estimation. An Applied Tutorial for Research Development, Test and Evaluation Engineers”, New York: IEEE, 1993.

[18] S. Prasad, M. S. Narayanan and S. R. Desaj, "Time Delay Estimation Performance in a Scattering Medium," IEEE Transactions on Acoustics Speech and Signal Processing, ASSP -33, pp. 50-60, February 1985

[19] K.C. Ho, Y. T. Chan, and R. J. Inkol, “Pulse Arrival time estimation Based on Pulse Sample Ratios”, IEE Proceedings of Radar Sonar and Navigation, vol. 142, pp. 153-157, August 1995

[20] D. J. Torrieri, “Arrival Time Estimation by Adaptive Thresholding”, IEEE Transactions on Aerospace and Electronics, AES-10, pp. 178–184, March 1974

[21] D. J. Torrieri, “The Uncertainty of Pulse Position due to Noise”, IEEE Transactions on Aerospace and Electronics, AES-8, pp. 661–668, March 1972

[22] H. L. V. Trees, “Detection, Estimation and Modulation Theory Volume I”, John Wiley and Sons, 2001

[23] J. G. Proakis, “Digital Communications”, Mc. Graw Hill, Inc., 3rd edition, 1995

[24] “Digital Land Mobile Radio Communications,” COST Telecom Secretariat, European Commission, Brussels, Belgium, COST 207, 1989.

[25] T. Taga and T. Tanaka, “Delay Spread Reduction Effect of Beam Antenna and Adaptively Controlled Beam Facing Access System in Urban Line-of-Sight Street Microcells”, IEEE Transactions on Vehicular Technology, Vol. 52, July 2003.

[26] T. W. H. Tranter, T. S. Rappaport, K. L. Kosbar and K. S. Shanmugan, “Principles of Communication Systems Simulation with Wireless Applications”, 1st edition, New Jersey, Prentice Hall, 2004.

[27] Jerry D. Gibson, “The Mobile Communications Handbook”, IEEE Press, 2nd edition, 1999

[28] G. L. Stüber, “Principles of Mobile Communication”, 2nd edition, Kluwer, 2002.

[29] D. Torrieri, “Principles of Spread-Spectrum Communication Systems”, Springer, 1st edition, 2004

[30] M. A. Richards, “Fundamentals of Radar Signal Processing”, Mc. Graw Hill, Inc., 1st edition, 2005

[31] S. Koç, “Radar Detectability and Jamming Effectiveness”, Aselsan Technical Report, 2005

[32] M. Streetly, “Jane’s Radar and Electronic Warfare Systems 2006-2007”, Jane’s Information Group, 2006

APPENDIX A

SYNCHRONIZATION ACCURACY FOR TDOA

AOA expression in terms of *TDOA*, distance between sensors, *d*, and speed of light, *c*, is given below:

$$AOA = \sin^{-1}\left(\frac{TDOA * c}{d}\right) \tag{A-1}$$

Let the AOA estimation tolerance to the time synchronization error be 0.05°. Since derivative of $\sin^{-1}()$ is increasing with increasing argument, for error of 0.05°, corresponding time synchronization error must be higher at angle close to 90°. So let desired AOA be 89.95°, then following expression would give the worst time synchronization error in order to make a 0.05° error.

$$\Delta TDOA = d\frac{(\sin(90°) - \sin(89.95°))}{c} \tag{A-2}$$

$\Delta TDOA$ is the time synchronization accuracy in order to have and AOA estimation tolerance of 0.05°. For d=750 m and c=3*10^{8}m/sn, required synchronization accuracy is $\Delta TDOA$=9*10^{-13} sec

If the angular coverage is limited to 40° as mentioned in section 6.2, then the synchronization accuracy drops to 1.7 nsec

APPENDIX B

DERIVATION OF AOA TDOA CRLB

Assume that we observe a pulse like signal and try to decide its time of arrival

$$r(t) = \sqrt{A}s(t - T_o) + n(t) \tag{B-1}$$

where $n(t)$ is white Gaussian noise and

$$s(t) = rect(t, T_p) = \begin{cases} 1 & , \quad -T_p/2 \le t \le T_p/2 \\ 0 & , \quad else \end{cases} \tag{B-2}$$

It is straightforward to show for any unbiased estimate of $\hat{T}_o$,[22]

$$\text{var}(\hat{T}_o - T_o) \ge \frac{N_o}{2\int_0^T \left[\frac{\partial s(t - T_o)}{\partial T_o}\right]^2 dt} \tag{B-3}$$

However, since s(t) is discontinuous the denominator becomes infinite and $CRLB(\hat{T}_o) = 0$. This is due to infinite bandwidth of the received signal which is not possible in practice.

Normally, we would have samples of $r(t)$ at the sampling instants, i.e.,

$$r_k = r(kT_s) = \sqrt{A}s(kT_s - T_o) + n(kT_s) \quad k = 0, \cdots, K \tag{B-4}$$

In fact, from the samples r_k, we can uniquely generate time signal $r_L(t)$ which is bandlimited to $-1/T_s \le f \le 1/T_s$, thus we may assume our observation is $r_L(t)=\sqrt{A}s_L(t-T_o)+n_L(t)$ where $n_L(t)$ is bandlimited noise with spectral height N_o over $-1/T_s \le f \le 1/T_s$. Again it is straightforward to show that

$$\mathrm{var}\left(\hat{T}_o - T_o\right) \ge \frac{N_o}{2\int_0^T \left[\frac{\partial s_L(t-T_o)}{\partial T_o}\right]^2 dT} \equiv CRLB\left(\hat{T}_o\right) \tag{B-5}$$

for any unbiased estimate $\hat{T}_o$

To have a good estimate of TOA, the observation time must include whole signal, then we must have $T >> T_p >> T_s$.

Hence we can write

$$I = \int_0^T \left[\frac{\partial s_L(t-T_o)}{\partial T_o}\right]^2 dT = \int_{-\infty}^{\infty} \left[\frac{\partial s_L(t-T_o)}{\partial T_o}\right]^2 dT = \int_{-\infty}^{\infty} \left|F\left\{\left[\frac{\partial s_L(t-T_o)}{\partial T_o}\right]\right\}\right|^2 df \tag{B-6}$$

$$\left|F\left\{\left[\frac{\partial s_L(t-T_o)}{\partial T_o}\right]\right\}\right|^2 = \left|\frac{\partial}{\partial T_o} S_L(f) e^{-j2\pi f T_o}\right|^2 = 4\pi^2 f^2 |S_L(f)|^2 =$$

$$\begin{cases} 4\pi^2 f^2 |S_L(f)|^2 & -1/T_s \le f \le 1/T_s \\ 0 & else \end{cases} \tag{B-7}$$

where $S(f) = F\{rect(t,T_p)\} = \sqrt{A}T_p \dfrac{\sin(\pi f T_p)}{\pi f T_p}$

Thus $I \approx \int_{-1/T_s}^{1/T_s} AT_p^2 4\pi^2 f^2 \frac{\sin^2(\pi f T_p)}{(\pi f T_p)^2} df$

Since $T_p >> T_s$, $I \approx \frac{4A}{T_s}$

Then CRLB for TOA estimation is $CRLB(\hat{T}_o) \approx \frac{N_o T_s}{8A}$

Since TDOA estimation is difference of TOA estimations of 2 signals given below:

$$\begin{aligned} r_1(t) &= \sqrt{A_1}\, s(t - T_1) + n_1(t) \\ r_2(t) &= \sqrt{A_2}\, s(t - T_2) + n_2(t) \end{aligned} \tag{B-8}$$

and the estimations are independent of each other CRLB for TDOA can be written as

$$\frac{N_o T_s}{8}\left(\frac{1}{A_1} + \frac{1}{A_2}\right) \tag{B-9}$$

In [6] it is shown that variance of TDOA can be related to variance of AOA estimation by following expression:

$$\sigma^2{}_{AOA} = \frac{\sigma^2{}_{TDOA}}{\left(\frac{d}{c}\right)^2 - (TDOA)^2} \tag{B-10}$$

where *d* is distance between sensors and *c* is the speed of light. Then CRLB for AOA estimation can be written as follows for $A=A_1=A_2$

$$CRLB(AOA) = \frac{\frac{N_o T_s}{4A}}{\left(\frac{d}{c}\right)^2 - (TDOA)^2} \tag{B-11}$$

APPENDIX C

CALCULATION OF PERFORMANCE METRICS

Let the AOA estimates obtained as a result of Monte Carlo simulations be $\theta_1 ... \theta_N$ and actual AOA be Ψ. Then mean, RMS error and standard deviation of the AOA estimates are given in Table C-1.

Table C-1: Calculation of performance metrics

Mean	$\frac{1}{N}\sum_{i=1}^{N}\theta_i$
Bias	$\Psi - \frac{1}{N}\sum_{i=1}^{N}\theta_i$
RMS error	$\sqrt{\frac{1}{N-1}\left(\sum_{i=1}^{N}\left(\theta_i - \Psi\right)^2\right)}$
Standard deviation	$\sqrt{\frac{1}{N-1}\left(\sum_{i=1}^{N}\left(\theta_i - \frac{1}{N}\sum_{i=1}^{N}\theta_i\right)^2\right)}$

APPENDIX D

MAXIMUM NUMBER OF DIVERSITY BRANCHES

For the assumption of TDOA between array elements in a sensor site being zero, $\frac{(N-1)d}{c} << \Theta$ where d is the distance between sensor in an array in a sensor site, N is the number of sensors in a sensor array and Θ is TDOA estimation resolution of the system. Then following expression can be written

$$10\frac{(N-1)d}{c} < \Theta \tag{D-1}$$

If the above expression is manipulated following expression is obtained:

$$N < \frac{\Theta * c}{10d} + 1 \tag{D-2}$$

Then for d 30 cm, TDOA resolution 0.1 μsec and wavelength 3 cm, maximum number of diversity antennas in the system is 10.

APPENDIX E

SMOOTHING OF THE CHANNEL WITH DIVERSITY

In order to show the smoothing of the channel, we have to show that the variance of the channel taps decrease as a result of diversity. Assume the following for simplicity:

- The detectors are linear
- Input to the channel is an impulse
- Channel is noiseless
- Receiver has N diversity channels

Then received signal can be written as follows:

$$\frac{1}{N}\sum_{k=1}^{N}\left|\sum_{i=1}^{K}a_{ki}\delta(t-iT_s)\right| \tag{E-1}$$

Where a_{ki} are complex Gaussian zero mean channel taps with variances σ_{ki}^2, K is the number of channel taps and N is number of diversity antennas

According to triangle inequality equation (E-1) can be written as:

$$\frac{1}{N}\sum_{k=1}^{N}\left|\sum_{i=1}^{K}a_{ki}\delta(t-iT_s)\right| \le \frac{1}{N}\sum_{i=1}^{K}\sum_{k=1}^{N}|a_{ki}|\delta(t-iT_s)=\sum_{i=1}^{K}b_i\delta(t-iT_s) \tag{E-2}$$

Assuming that $\sigma_{1i}^2 = \sigma_{2i}^2 = \cdots = \sigma_{Ni}^2$, if variance of b_i, $Var\{b_i\}$ is shown to be equal to $\frac{Var\{|a_{1i}|\}}{N}$ then the proof will be complete.

Variance of b_i can be written in terms of variance of $|a_{1i}|$ as follows:

$$
\begin{aligned}
& Var\{b_i\} = E(b_i^2) - (E(b_i))^2 = \\
& = \frac{1}{N^2}\left\{ E\left(\left(\sum_{k=1}^{N} |a_{ki}| \right)^2 \right) - E\left(\left(\sum_{k=1}^{N} |a_{ki}| \right) \right)^2 \right\} \\
& = \frac{1}{N^2}\left\{ NE(|a_{1i}|^2) + (N-1)(N)(E(|a_{1i}|)^2) - (N)^2 (E(|a_{1i}|)^2) \right\} \qquad \text{(E-3)} \\
& = \frac{1}{N}\left(E(|a_{1i}|^2) - E(|a_{1i}|)^2 \right) \\
& = \frac{1}{N} Var\{|a_{1i}|\}
\end{aligned}
$$

Then (E-3) shows that the variance of channel taps decrease when the diversity is applied.